



5 **Leaf Area Index Changes Explain GPP Variation across an
Amazon Drought Stress Gradient**

Sophie Flack-Prain¹, Patrick Meir^{1,2}, Yadvinder Malhi⁴, Thomas Luke Smallman^{1,3}, Mathew
Williams^{1,3}

¹ School of GeoSciences, University of Edinburgh, Edinburgh, UK

10 ² Research School of Biology, Australian National University, Canberra, ACT, Australia

³ National Centre for Earth Observation, University of Edinburgh, UK

⁴ Environmental Change Institute, School of Geography and the Environment, University of Oxford,
Oxford, UK

Correspondence to: Sophie Flack-Prain (s.flack-prain@ed.ac.uk)

15

20

25



Abstract

30 The capacity of Amazon forests to sequester carbon is threatened by climate change-induced shifts in precipitation patterns. However, the relative importance of plant physiology, ecosystem structure, and trait composition responses in determining variation in GPP, remain largely unquantified, and vary among models. We evaluate the relative importance of key climate constraints to gross primary productivity (GPP), comparing direct plant physiological responses to water availability and indirect
35 structural and trait responses (via changes to leaf area index (LAI), roots and photosynthetic capacity). To separate these factors we combined the Soil-Plant-Atmosphere model with forcing and observational data from seven intensively studied forest plots along an Amazon drought stress gradient. We also used machine learning to evaluate the relative importance of individual climate factors across sites. Our model experiments showed that variation in LAI was the principal driver of differences in GPP across
40 the gradient, accounting for 33% of observed variation. Differences in photosynthetic capacity (V_{cmax} and J_{max}) accounted for 21% of variance, and climate (which included physiological responses) accounted for 16%. Sensitivity to differences in climate was highest where shallow rooting depth was coupled with high LAI. On sub-annual timescales, the relative importance of LAI in driving GPP increased with drought stress ($R^2=0.72$), whilst the importance of solar radiation decreased ($R^2=0.90$).
45 Given the role of LAI in driving GPP across Amazon forests, improved mapping of canopy dynamics is critical, opportunities for which are offered by new satellite-based remote sensing missions such as GEDI, Sentinel and FLEX.

Keywords: Canopy Dynamics, Leaf Traits, Tropical Rainforests, Precipitation, Gross Primary
50 Productivity



55 1. Introduction

As the entry point for carbon into the biosphere, gross primary productivity (GPP) is central to the global carbon cycle. Tropical rainforests alone account for one third of total terrestrial photosynthesis assimilating ~41 Pg of carbon each year (Beer et al., 2010). Carbon fluxes across the tropics are tightly coupled to climate, and water availability is a principal driver of spatial and temporal variation in photosynthesis (Fisher et al., 2007, Von Randow et al., 2013, Beer et al., 2010, Malhi et al., 2015, Guan et al., 2015). Across Amazon forests, GPP decreases linearly with increasing seasonal water deficit (Malhi et al., 2015). Shifts in precipitation patterns as a result of anthropogenic climate change are predicted to have a major impact on Amazon GPP (Phillips et al., 2009, Malhi et al., 2008, Meir and Woodward, 2010, Zhang et al., 2015, Meir et al., 2015a). Longer and more intense dry seasons are projected, together with an increased frequency and severity of drought events (Joetzjer et al., 2013, Boisier et al., 2015, Duffy et al., 2015). Given the biogeochemical influence of Amazon forests at regional and global scales (Liu et al., 2017), accurately predicting GPP response to drought stress is critical.

Dynamic global vegetation models (DGVMs) disagree on the effects of projected precipitation change on Amazon carbon dynamics. Galbraith et al. (2010) found future shifts in precipitation patterns had little effect on model estimates of biomass change (for two of the three models tested), reflecting poorly the observed sensitivity of Amazon forests to water availability illustrated by through-fall exclusion experiments and natural drought events (Rowland et al., 2015a, Nepstad et al., 2007, Phillips et al., 2009). Substantial progress has been made in model development to capture the impact of drought stress on plant physiology. By coupling stomatal conductance and plant hydraulic theory, models have proved better able to predict ecosystem functioning and mortality (Eller et al., 2018, Fisher et al., 2018, Fisher et al., 2006, Fisher et al., 2007, Bonan et al., 2014). However, the interactions between drought stress, ecosystem structure (e.g. canopy dynamics and rooting depth) and trait composition (e.g. V_{cmax} , J_{max} , leaf lifespan and leaf mass per unit area (LMA)), are typically absent from models, despite having a major impact on simulated GPP (Fauset et al., 2012, Sakschewski et al., 2016, Lee et al., 2013).



Furthermore, changes in canopy dynamics have been identified as a likely cause for the disparity between field observations and model predictions (Restrepo-Coupe et al., 2017, Powell et al., 2013).

The relative importance of plant physiology, ecosystem structure, and trait composition responses in determining variation in GPP, remain largely unquantified in data-constrained analysis (Meir et al., 85 2015b). Plant physiological responses to drought stress include stomatal conductance, which is limited by water availability and atmospheric demand. Stomatal conductance constrains GPP via changes in CO₂ supply, but is considered a short (varying on sub-hourly timescales), rather than long-term response to climate forcings (Sperry et al., 2002). Changes to ecosystem structure and traits, such as LAI, rooting depth and carboxylation capacity, are expected to be more longstanding (Meir et al., 2015a).

90 Extensive evidence links spatial and temporal variation in drought stress with ecosystem structure. Leaf area index (LAI) typically decreases with increasing drought stress (Iio et al., 2014, Meir et al., 2015b, Brando et al., 2008, Grier and Running, 1977, Wright et al., 2013). LAI determines the surface area for GPP, impacting light capture capacity. Near surface root mass, length and surface area decline with seasonal drought stress (and increase during periods of high soil water availability to exploit available 95 resources), whilst deep roots can support water supply during dry periods (Nepstad et al., 1994, Metcalfe et al., 2008). Root depth, mass and traits influence hydraulic supply and consequently stomatal conductance.

Leaf traits similarly exhibit spatial and temporal variation with changing water availability. Leaf nitrogen content (per unit mass), light- and CO₂-saturated photosynthetic rates (per unit mass) increase 100 with drought stress across tropical precipitation gradients, whilst p₅₀ (the water potential at which 50% of hydraulic conductivity is lost) declines (Wright et al., 2004, Santiago et al., 2004, Anderegg, 2015). Leaf traits affect GPP via photosynthetic capacity (V_{cmax} and J_{max}) (Bahar et al., 2017, Fyllas et al., 2017), and through their influence on canopy carbon economics, via leaf growth and maintenance costs (Bloom et al., 1985). However, understanding the interactions between photosynthetic drivers across 105 different spatial and temporal scales is limited.



Field observations show variation in Amazon GPP is correlated with physiological, ecosystem structure and trait composition responses to climate (Restrepo-Coupe et al., 2013, Goulден et al., 2004, Hutyrа et al., 2007, Wu et al., 2017, Wagner et al., 2017). Modelling approaches have similarly highlighted the role of canopy dynamics and leaf traits in driving spatial and temporal variation in GPP (Mercado et al., 2011, Castanho et al., 2013, Restrepo-Coupe et al., 2013, Rodig et al., 2018), however their relative effects have not been explicitly isolated and quantified. Quantifying the direct effect of discrete photosynthetic drivers has been limited by the need for detailed field measurements of carbon fluxes, canopy dynamics and traits. Furthermore, whilst a deserved research effort has focused on the importance of nutrient availability in driving spatial variation in GPP (Mercado et al., 2011, Castanho et al., 2013), the role of ecosystem responses to water availability has received less attention (Green et al., 2019). In light of projected changes in rainfall patterns across the basin, capturing responses to water availability in ecosystem models is critical to reducing current uncertainty around Amazon climate-vegetation feedbacks. We aim to reduce the uncertainty by assessing the relative effects of physiological, structural and trait responses to water availability on GPP across monthly to annual timescales.

We apply a validated ecosystem model to plots across the Amazon, spanning a large drought stress gradient, and a range in forest types from moist equatorial to seasonally dry tropical forests. Process modelling allows the links between climate, ecosystem structure and leaf traits to be quantified explicitly, and separated, across timescales (Figure 1). The soil plant atmosphere model (SPA) (Williams et al., 1996, Williams et al., 1998, Fisher et al., 2006, Fisher et al., 2007, Rowland et al., 2015b) is well suited to this investigation given its prior use in accurately simulating carbon and water fluxes in Amazon tropical forests. We link the modelling to data gathered over multiple years (2009-2010) on permanent sample plots from the Global Ecosystems Monitoring (GEM) network (Doughty et al., 2015a, Malhi et al., 2015). The datasets comprise detailed measurements of carbon fluxes, carbon stocks and leaf traits, and were used to constrain the SPA model. We simulate the effect of forest structure and leaf trait distributions along the drought stress gradient, and explore the covariation of



observed leaf traits (leaf N content (a proxy for photosynthetic capacity) and LMA) and those derived from model calibrations (leaf lifespan), before using SPA to address the following questions:

1. Is spatial variation in GPP across the drought stress gradient principally driven by the direct
135 effects of climate and soils, which include physiological responses to water availability via hydraulic transport and stomatal conductance? Alternatively, are indirect effects of climate, via structural and trait responses to water availability (LAI, rooting biomass, root depth and photosynthetic capacity i.e V_{cmax} and J_{max}), more important?
2. Does the sensitivity of GPP to differences in climate, LAI, photosynthetic capacity (V_{cmax} and
140 J_{max}) and rooting depth vary across the drought stress gradient?
3. What drives seasonal variation in GPP across an Amazon forest drought stress gradient?

Linked to question one, we hypothesise that indirect effects of climate via structural and trait responses are more important than the direct effects (via physiological responses), in explaining spatial variation in GPP across the drought stress gradient (Figure 1). We further posit that LAI is the principal driver
145 of differences in GPP among Amazon forests, effected through the observed increase in leaf area with decreasing drought stress.

For question two, we predict that the sensitivity of GPP to differences in climate, LAI, photosynthetic capacity (V_{cmax} and J_{max}) and rooting depth will vary dependent on water demand (via LAI and stomatal conductance) and supply (climate and root depth and biomass; Figure 1). We expect that forests under
150 lower drought stress will be most sensitive to differences in LAI and photosynthetic capacity within the bounds of observations across the gradient. We predict that forests under higher drought stress will be more sensitive to differences in rooting depth. We expect forests with high LAI but shallow rooting depth will be most sensitive to differences in climate, due to their higher transpiration demand but low capacity for water supply.

155 For question three, we hypothesise that on monthly timescales, climate will be more important than canopy dynamics in driving GPP. Across the drought stress gradient, we expect that solar radiation will be relatively more important during the wet season, whilst VPD will be more important during the dry season, reflecting seasonal shifts in light and water availability. Due to differences in dry season length,



we predict that for forests experiencing lower drought stress, solar radiation will be most important in driving sub-annual variation in GPP, whilst for forests under higher drought stress, VPD will be the dominant driver.

By combining detailed plot-level timeseries data with a hydrodynamic terrestrial ecosystem model, we are able to use an innovative model experimentation approach to understand the drivers of spatial variation in GPP, beyond correlative effects. We are able to apportion variation in GPP to the direct and indirect effects of climate (Figure 1), across sub-annual and annual timescales (Q1 and Q3). Furthermore, by performing a sensitivity analysis within the context of observed variation in parameters across the Amazon (Q2) we identify areas potentially more vulnerable to changes in precipitation regime.

2. Methods

We parameterised and validated the ecosystem model SPA to permanent sample plots along an Amazon mean Maximum Climatological Water Deficit (MCWD) gradient (-85 to -498 mm yr⁻¹) for the years 2009-2010. Plot characteristics are summarised in Table 1, and detailed in full in the supplementary material. MCWD is a measure of peak seasonal water deficit, where more negative MCWD indicate higher drought stress. We used MCWD instead of annual precipitation as water deficit is more closely linked to mechanisms constraining GPP than total water input. We analysed the distribution of LAI and leaf traits across the MCWD gradient. We then undertook a series of model experiments to: (i) apportion spatial variation in GPP to drivers (climate, soils, LAI, rooting biomass and depth and photosynthetic capacity); (ii) investigate how the sensitivity of GPP to differences in drivers varies across the MCWD gradient; and (iii) quantify the importance of LAI, VPD, solar radiation, precipitation and air temperature in driving sub-annual variation in GPP using the random forest machine learning technique (Breiman, 2001).

2.1 The Soil Plant Atmosphere model (SPA)

The Soil-Plant-Atmosphere model (SPA) is a hydrodynamic terrestrial ecosystem model, which has been calibrated and evaluated for moist tropical forests in Manaus and Caxiuanã (Williams et al., 1996, Williams et al., 1998, Fisher et al., 2007). In SPA, carbon and water fluxes are estimated through



process-based modelling of radiative transfer, boundary layer and stomatal conductance, plant and leaf ecophysiology and soil-plant energy and water balance (Smallman et al., 2013, Williams et al., 1996). Plant physiological responses to water availability are well represented in SPA due to the stomatal conductance algorithm being coupled directly to plant water use (Fisher et al., 2006). Within SPA, C allocation between structural tissue and the non-structural C (NSC) pool is executed via the sub model DALEC_{canopy} (Bloom and Williams, 2015) (Figure 2). Leaf maintenance respiration was calculated as a function of leaf N content (Reich et al., 2008) and total leaf C stock (see supplementary material). Within SPA, wood and fine root maintenance respiration were simulated as a function of component C stock and a plot specific respiration coefficient. Growth respiration was calculated as fixed fraction of NPP (0.28) (Waring and Schlesinger, 1985).

2.2 Model Calibration

Following data collation to parameterise SPA, the model was calibrated and validated for each plot prior to conducting model experiments. Measurements used to parameterise SPA include: soil texture, soil C stock, leaf N content, LMA, photosynthetic capacity, the fraction of NPP allocated to fine roots and wood, root depth, and foliar, wood and fine root C stocks (Table 2). Soil, wood and fine root C stocks (single point measurements, not timeseries) were initial model inputs and allowed to vary thereafter dependent on simulated C dynamics. Plot specific field measurements of leaf N content are presented in Fyllas et al. (2009), or where absent were retrieved from trait databases using plot species composition (Kattge et al., 2011; Poorter and Bongers, 2006). Photosynthetic capacity estimates (V_{cmax} and J_{max}) were derived from leaf N content (Walker et al., 2014), or field measurements (Caxiuanã only). Wood and root respiration measurements were used together with component C stocks to estimate plot specific wood and root respiration coefficients.

The model was driven using hourly meteorological data, retrieved from local weather stations. Short gaps in air temperature, wind speed, shortwave radiation and vapour pressure deficit measurements (<6 hours), were filled by spline interpolation between existing data. Where local meteorological data was unavailable for a longer period of time, or for gaps in precipitation measurements, hourly spline-interpolated ERA-Interim data were used (Dee et al., 2011). The interpolation of solar radiation



estimates accounted for the solar zenith angle. MCWD was calculated for the years 2009-2010 as the minimum monthly water deficit reached within the year, where monthly water deficit is equal to the
215 previous month's water deficit, plus precipitation, minus evapotranspiration (Aragao et al., 2007).
Calculated MCWD was consistent with previously published estimates for all plots excluding Caxiuanã,
which were calculated across different years (Malhi et al., (2015), Caxiuanã -203mm, Tambopata -
259mm, Kenia -386mm, Tanguro -482mm; this study, Caxiuanã -85±65mm, Tambopata -265±59mm,
Kenia 342±146mm, Tanguro 451±73mm).

220 The simulation of soil water drainage in SPA was calibrated against timeseries of field measurements
of soil moisture. Initial investigations comparing modelled soil moisture to monthly field data
highlighted an overestimation by SPA. The empirical model used in SPA to relate soil texture to water
retention (Saxton et al., 1986, eqn. 10) was then calibrated by adjusting the slope of the interaction to
better represent soil moisture across tropical soils (to within standard error estimates of mean annual
225 soil moisture).

Leaf litterfall parameters (day of peak leaf fall, leaf fall period and leaf lifespan) were calibrated against
field data to accurately simulate litterfall period and amplitude (within standard error estimates of
annual litterfall). Wood and fine root biomass turnover rates were estimated assuming each forest
ecosystem was at steady state given the maturity of stands and their disturbance history:

230
$$turnover\ rate_i \propto \frac{NPP_i}{C\ stock_i}$$

Where i is wood or fine roots.

Local LAI estimates derived from hemispherical photographs were used to force simulated LAI. Leaf
NPP was calculated as the difference between the foliar C stock of the previous timestep and that which
would equate to field measured LAI. Leaf NPP was allocated prior to other plant components, and if
235 the leaf NPP requirement exceeded total NPP for the given timestep, the non-structural C pool was
drawn upon (where total NPP was calculated as the difference between simulated GPP and autotrophic
respiration) (see supplementary material). Under the assumption that allocation to NSC is an active



process and that the pool serves functions additional to the seasonal redistribution of C (Dietze et al., 2014), depletions in the NSC pool induce redirection of a fraction of NPP towards NSC storage to
240 maintain a stable NSC pool. Root and wood NPP were calculated from the NPP remaining after leaf allocation.

2.3 Model Validation

For each plot, SPA calibrations were constrained by the upper and lower sample error of LAI measurements to produce an estimate of model uncertainty. However, given we do not quantify
245 intrinsic model error beyond that associated with parameter estimates, we recognise that the model error estimates presented are underestimated. Observation constrained SPA simulations were then validated against biometric field measurements of C fluxes (i.e. from infra-red gas analysers, dendrometers, root ingrowth cores litterfall traps etc.). Linear regression models were constructed to compare modelled estimates and independent field measurements of GPP, autotrophic respiration and total NPP. A
250 comprehensive comparison of model estimates and independent field measurements of component NPP and respiration were also made. Validation of the SPA model against biometric data lent confidence to subsequent analyses, where the model was used to explore C fluxes under non-observed conditions.

2.4 Model Experiments

Our aim was to isolate the direct effects of climate and soils (via physiological responses), ecosystem
255 structure, and leaf traits on simulated GPP. To avoid capturing the feedback effects of changing photosynthate supply (i.e. as a result of changes in climate, soils, ecosystem structure or traits) on ecosystem structure, model experiments were conducted in the absence of C cycle feedbacks. Thus, within model experiments, C stocks for each component (leaves, wood, fine root, coarse root) were constrained to observations unless otherwise stated.

260 2.4.1 Experiment 1. Drivers of Spatial Variation in GPP

Through a series of model input alternations, we used SPA to quantify the effects of (i) climate, (ii) soil properties, (iii) LAI, (iv) root biomass and (v) rooting depth, and (vi) trait responses driven by photosynthetic capacity (V_{max} and J_{max}), on simulated GPP. Model inputs for each driver were alternated at each plot, to that of all other plots, and annual GPP values for each of the two years



265 retrieved. For example, plot CAX04 was simulated with the climate, soil properties, LAI, root biomass,
root depth and photosynthetic capacity of CAX06, TAM05, TAM06, KEN01, KEN02, and Tanguro
etc. SPA simulated GPP for a total of 462 combinations (for climate, 7 plots \times 3 alternations \times 2 years,
plus for the remaining drivers, 5 drivers \times 7 plots \times 6 alternations \times 2 years) were combined with 14
annual GPP estimates from observation constrained (control) runs (7 plots \times 2 years). A factorial
270 ANOVA was applied to the difference between GPP from each model run and its control simulation
($n=476$, i.e. $462 + 14$) (Galbraith et al., 2010). The proportions of variation in GPP explained by climate,
soil properties, LAI, photosynthetic capacity, root biomass and rooting depth, were then calculated as
the conditional sum of square divided by the total sum of squares.

2.4.2 Experiment 2. Variation in Forest Sensitivity to Drivers of GPP

275 We quantified how the relative sensitivity of GPP to differences in LAI, climate, photosynthetic
capacity and rooting depth varied across the MCWD gradient. For example, we tested whether forests
occupying lower drought stress zones were more sensitive to differences in LAI than forests in higher
drought stress zones, etc. We used model outputs generated in *Experiment 1* to calculate the sensitivity
of GPP to drivers at each plot, within the bounds of observations across the MCWD gradient. Root
280 biomass and soil properties were not included in the analysis as across the MCWD gradient they
explained little variation in GPP (*Experiment 1*, Table 6). The sensitivity of GPP to drivers at each plot
was calculated as the absolute range in simulated GPP values under each driver alternation i.e. the
sensitivity of CAX04 to variation in LAI was calculated as the maximum GPP minus the minimum
GPP simulated by alternating LAI to that of all other plots etc. Plots were grouped by location
285 (Caxiuanã, Tambopata, Kenia and Tanguro) to compare how the sensitivity of GPP to LAI, climate,
photosynthetic capacity and rooting depth varies across the MCWD gradient.

2.4.3 Experiment 3. Drivers of Sub-Annual Variation in GPP

We quantified the role of climate and LAI in explaining variation in sub-annual GPP. We used the
random forest technique to compute the relative importance of LAI, VPD, solar radiation, precipitation
290 and air temperature driving variation in monthly GPP ($n=168$; 7 plots \times 24 months), where GPP
estimates were derived from SPA simulations. To quantify the effects of LAI and climate variables on



monthly GPP we used the random forest machine learning technique applied by means of the Python Scikit-Learn module (Breiman, 2001, Pedregosa et al., 2011). The approach uses multiple mathematical decision tree predictors to describe a dependent variable as a function of selected independent variables.

295 An importance value between 0 and 100 was assigned to each driver based on a tree-wise comparison of explanatory power (Moore et al., 2018, López-Blanco et al., 2017). We calculated the average relative importance of drivers at each plot to determine the principal drivers of variation in sub-annual GPP and investigated the seasonality of driver importance.

3. Results

300 Following model calibration, validation and an investigation into the distribution of LAI and leaf traits across the MCWD gradient, we (i) quantify the drivers of spatial variation in GPP, (ii) compute the variation in forest sensitivity to drivers of GPP, and (iii) calculate the relative importance of drivers of sub-annual variation in GPP.

3.1 Model Calibration

305 Calibrated SPA soil water content corresponded well to field measurements from the GEM network (Figure 3). Simulated mean annual soil moisture estimates were within field measurement standard error for all plots. The timing of observed peak soil moisture was captured by SPA simulations ($R^2=0.98$, $p<0.001$, RMSE=1 month). SPA simulated seasonal soil moisture range exhibited a non-significant, positive correlation with field measurements ($R^2=0.35$, $p=0.21$, RMSE=5%). Notably, for some plots
310 such as Kenia, the magnitudes of seasonal peak soil water fluxes were not captured by SPA simulations (up to 39% lower than field estimates), whilst for Tanguro, peak soil water lasted 3 months longer in SPA simulations than was measured in the field.

SPA was also successfully calibrated to simulate local leaf litterfall accurately. The calibration of leaf fall cycle parameters in SPA using GEM leaf litterfall timeseries (Table 4), resulted in the magnitude
315 and timing of leaf litterfall being well represented by the model for all plots (monthly leaf litterfall range for GEM measurements and SPA simulations $R^2=0.54$, $p=0.009$, RMSE= 11.2 gC m⁻² yr⁻¹; timing of



leaf litterfall peak $R^2=0.96$, $p<0.001$, $RMSE=1.1$ months) (Figure 4). SPA-simulated mean annual leaf litterfall correlated significantly with GEM estimates ($R^2=0.99$, $p<0.001$, $RMSE=9.0$ $gC\ m^{-2}\ yr^{-1}$).

3.2 Model Validation

320 Estimates of ecosystem-scale C fluxes from SPA model runs were validated against biometrically derived estimates from the GEM network. GPP_{SPA} and GPP_{GEM} estimates were correlated across plots, though not significantly ($R^2=0.36$, $p=0.15$; Figure 5a). Along the MCWD gradient, GPP_{SPA} estimates varied across plots by $1137\ gC\ m^{-2}\ yr^{-1}$, whilst GPP_{GEM} estimates varied by $1202\ gC\ m^{-2}\ yr^{-1}$. Error bars overlap between GPP_{SPA} and GPP_{GEM} estimates for all plots except KEN01 and TAM06, though
325 marginally (difference KEN01 $115\ gC\ m^{-2}\ yr^{-1}$, TAM06 $50\ gC\ m^{-2}\ yr^{-1}$). GPP_{GEM} error bars are field estimate standard error, and GPP_{SPA} error bars represent simulated GPP variance under LAI standard error. Across plots, GPP_{SPA} estimates were 0.57% higher than GPP_{GEM} estimates. The correlation between GPP and MCWD was similar for GPP_{SPA} ($R^2=0.64$, $p=0.03$, slope=2.4) and GPP_{GEM} estimates ($R^2=0.52$, $p=0.07$, slope=2.00).

330 NPP_{SPA} estimates (the sum of model simulated root and wood NPP and data-constrained leaf NPP) were also correlated with NPP_{GEM} measurements across plots ($R^2=0.38$, $p=0.14$), though not significantly due to differences in Kenia plots (on exclusion of Kenia plots $R^2=0.92$, $p=0.01$, $RMSE=42\ gC\ m^{-2}\ yr^{-1}$) (Figure 5b). NPP_{SPA} estimates were 7.9% lower than field measurements across plots on average. R_{SPA} (the sum of predicted leaf respiration, and parameterised root and wood respiration) were significantly
335 correlated with biometric measurements (R_{GEM}) across plots ($R^2=0.59$, $p=0.04$; Figure 5c), though were on average 5.3% higher.

Leaf respiration estimates simulated as a function of leaf nitrogen content were correlated with field measurements, though not significantly ($R^2=0.47$, $p=0.09$; Table 5). Parameterised wood and fine root respiration, together with fine root NPP, correlated significantly with field measurements. SPA
340 estimates of wood NPP did not correlate significantly with GEM measurements due to underestimation at KEN01 (on exclusion $R^2=0.78$, $p=0.02$, $RMSE=7.5\ gC\ m^{-2}\ yr^{-1}$). Further comparisons of SPA estimates and GEM measurements of component NPP and respiration are presented in Table 5.



3.4 LAI and Leaf Traits Trends along the MCWD gradient

Field estimated mean annual LAI ranged from 2.2 to 5.2 m² m⁻², and increased (though not significantly) with MCWD across plots ($R^2=0.35$, $p=0.16$). A negative, non-significant correlation existed between calibrated leaf lifespan and MCWD ($R^2=0.50$, $p=0.08$). Photosynthetic capacity (V_{cmax} and J_{max}) estimates derived from measured leaf N content similarly exhibited a negative non-significant correlation with MCWD ($R^2=0.51$, $p=0.07$ and $R^2=0.53$, $p=0.06$ respectively). A positive non-significant correlation existed between model-calibrated leaf lifespan, measured LMA (log-log $R^2=0.39$, $p=0.14$), and LAI ($R^2=0.28$, $p=0.22$). Model-calibrated leaf lifespan exhibited a negative non-significant correlation with photosynthetic capacity estimates (V_{cmax} $R^2=0.46$, $p=0.09$; J_{max} $R^2=0.47$, $p=0.09$). A significant positive correlation existed between mean annual LAI and LMA ($R^2=0.85$, $p=0.003$).

3.5 Model Experiments

3.5.1 Experiment 1. Drivers of Spatial Variation in GPP

Structural and trait responses to water availability explained more variation in GPP across the MCWD gradient than did climate. LAI accounted for the largest proportion of variance in mean annual GPP across plots (32.8%), whilst 21.3% was explained by differences in photosynthetic capacity (Table 6). Photosynthetic capacity increased with decreasing MCWD (Table 3); this relationship partially offset the decrease in GPP linked to declining LAI. The direct effects of climate on GPP (which included physiological responses to water availability including stomatal conductance) accounted for 16.2% of plot variation in mean annual GPP. Rooting depth did not vary directionally with MCWD and consequently only had a small effect on GPP (4.1%). Soil properties and root biomass accounted for a very small fraction of variance (<2%).

3.5.2 Experiment 2. Variation in Forest Sensitivity to Drivers of GPP

The relative sensitivity of GPP to drivers varied across the MCWD gradient (Figure 6). GPP was most sensitive to changes in LAI (per unit m² leaf area) for plots located at Caxiuanã, which experience the least negative MCWD and have large rooting depth (Caxiuanã LAI sensitivity Δ 537 gC m⁻² yr⁻¹ vs



overall mean LAI sensitivity $\Delta 380 \text{ gC m}^{-2} \text{ yr}^{-1}$). The sensitivity of GPP to LAI exhibited a positive, non-significant correlation with MCWD ($R^2=0.88$, $p=0.06$; Tanguro LAI sensitivity $\Delta 286 \text{ gC m}^{-2} \text{ yr}^{-1}$, Kenia $\Delta 345 \text{ gC m}^{-2} \text{ yr}^{-1}$, Tambopata $\Delta 353 \text{ gC m}^{-2} \text{ yr}^{-1}$). Reflecting LAI trends, the sensitivity of GPP to differences in photosynthetic capacity (per unit $\mu\text{mol C g s}^{-1}$) was similarly highest at Caxiuanã (Caxiuanã photosynthetic capacity sensitivity $\Delta 27 \text{ gC m}^{-2} \text{ yr}^{-1}$, mean photosynthetic capacity sensitivity $\Delta 20 \text{ gC m}^{-2} \text{ yr}^{-1}$; Table 3), and decreased linearly (though not significantly) across the MCWD gradient ($R^2=0.83$, $p=0.09$; Tanguro photosynthetic capacity sensitivity $\Delta 16 \text{ gC m}^{-2} \text{ yr}^{-1}$, Kenia $\Delta 18 \text{ gC m}^{-2} \text{ yr}^{-1}$, Tambopata $\Delta 18 \text{ gC m}^{-2} \text{ yr}^{-1}$). Tambopata plots, which have high LAI but shallow rooting depth, were most sensitive to differences in climate (per unit MCWD mm) ($3.44 \text{ gC m}^{-2} \text{ yr}^{-1}$), whilst Kenia plots, which have similarly shallow rooting depth but low LAI, were the least sensitive (Kenia climate sensitivity $\Delta 1.64 \text{ gC m}^{-2} \text{ yr}^{-1}$, Tanguro $\Delta 2.77 \text{ gC m}^{-2} \text{ yr}^{-1}$, Caxiuanã $\Delta 1.78 \text{ gC m}^{-2} \text{ yr}^{-1}$). The sensitivity of GPP to differences in rooting depth (per m rooting depth) was highest at Tanguro and Tambopata (Tanguro rooting depth sensitivity $\Delta 114 \text{ gC m}^{-2} \text{ yr}^{-1}$, Tambopata $\Delta 79 \text{ gC m}^{-2} \text{ yr}^{-1}$), and lowest at Caxiuanã and Kenia (Caxiuanã rooting depth sensitivity $\Delta 28 \text{ gC m}^{-2} \text{ yr}^{-1}$, Kenia $\Delta 20 \text{ gC m}^{-2} \text{ yr}^{-1}$).

3.5.3 Experiment 3. Drivers of Sub-Annual Variation in GPP

In contrast to drivers of spatial variation in GPP, on a sub-annual timescale LAI had less explanatory power than climate (Tables 6 and 7). The relative importance of solar radiation in driving monthly GPP increased significantly with MCWD ($R^2 = 0.90$, $p < 0.001$), whilst the relative importance of LAI declined ($R^2=0.72$, $p=0.015$). The relative importance of VPD did not vary directionally across the MCWD gradient ($R^2=0.10$, $p=0.49$). Both precipitation and air temperature had little effect on monthly GPP, though it is noted that a significant interaction existed between both precipitation and VPD ($p < 0.001$) and air temperature and shortwave radiation ($p < 0.001$). Furthermore, temperature varied least across plots in comparison to other climate forcings (standard deviation as a percentage of the mean; temperature 9.8%, VPD 73%, precipitation 192%, shortwave radiation 34%). As such, seasonal changes in the relative importance of temperature and precipitation were not investigated further. The relative importance of LAI, VPD and solar radiation shifted seasonally, reflecting changes in the availability of light and water. Solar radiation was typically the most important driver of monthly GPP during the wet



season, whilst VPD was more important during the dry season (Figure 7). The relative importance of LAI forcings peaked before dry season onset for forests under lower drought stress (Caxiuana and Tambopata), and during the dry season for forests under higher drought stress (Kenia and Tanguro). Notably, LAI was also more important during the dry season at KEN02, which occupies shallow soil (<1 m) in comparison to KEN01.

4. Discussion

Our aim was to better understand the mechanisms coupling GPP and drought stress across Amazon forests. We found that, leaf traits (both modelled and observed) and LAI co-varied along the MCWD gradient. Across observed ranges in key variables, LAI was the principal driver of spatial variation in GPP, followed by photosynthetic capacity (Q1). Forest sensitivity to differences in LAI and photosynthetic capacity decreased with increasing drought stress (Q2). Forests with higher evaporative potential (high LAI) relative to water supply were most sensitive to differences in climate and rooting depth. Solar radiation was a key driver of sub-annual variation in GPP, the relative effect of which increased with decreasing drought stress, coincident with declines in the relative importance of LAI, consistent with the evaluation from the sensitivity analysis (Q3).

4.1 LAI and Leaf Traits along the MCWD gradient

Leaf trait parameters retrieved from SPA litterfall calibrations suggest a wide range of potential leaf lifespans across the MCWD gradient (~1-3 years), and are in accordance with estimates for Amazon tree species, reported by Reich et al. (1991) of between two months and four years (Table 4). Leaf trait estimates co-varied across the MCWD gradient, in line with leaf economic theory (Wright et al., 2004). However, the interactions were often not significant. We suggest that in instances where R^2 values indicate a large proportion of variation is explained, high p-values may have occurred as a result of a small sample size (i.e. 7 plots). As drought stress increased, a shift towards deciduous strategies resulted in reduced leaf lifespan, but higher photosynthetic capacity. The co-variation of leaf traits along the MCWD gradient shapes both the rate of carbon assimilation (via photosynthetic capacity), and the carbon economics of canopy dynamics (via LMA, leaf lifespan and metabolic rate). Coincident with



changes in leaf traits, mean annual LAI increased with decreasing drought stress. Whilst research efforts have focused on mapping LAI (Iio et al., 2014) and leaf trait (Kattge et al., 2011, Asner et al., 2015) distributions across climatic gradients, their covariance has not yet been explored. Given the role of leaf
425 traits in shaping canopy carbon economics, the mechanisms underpinning LAI and leaf trait distributions across the resource availability gradient could prove important in understanding the effect of changes in precipitation regime on future Amazon carbon dynamics.

4.2 Drivers of Spatial Variation in GPP

Indirect effects of climate via ecosystem structure and long-term trait responses to water availability
430 accounted for 54% of variation in GPP (Q1; Figure 1). Direct effects of climate (which included physiological responses to water availability) accounted for only 16% of observed variance (Table 6). Our results are consistent with previous reports on the importance of ecosystem structure and traits in determining spatial variation in GPP (Rodig et al., 2018, van de Weg et al., 2013, Reichstein et al., 2014), but go further to quantify the direct contribution of discrete drivers to observed variation in
435 carbon assimilation. LAI explained the greatest proportion of variation in GPP, followed by photosynthetic capacity, whilst root and soil properties had little explanatory power.

Evidence of changes in LAI in response to precipitation regime has been presented across multiple ecosystems and over time (Grier and Running, 1977, Schleppi et al., 2011, Iio et al., 2014, Dobbertin et al., 2010, Wright et al., 2013). Amazonian forest throughfall exclusion experiments identified a
440 decline in LAI with the onset of reduced soil water (Fisher et al., 2007, Meir et al., 2008, Brando et al., 2008). At Caxiuanã, over a 4-year period, observed leaf area was 20-30% lower than the control stand (Meir et al., 2009), with long-term reductions estimated at between 10-15% (Rowland et al., 2015a). Investigations show that declines in LAI are not caused by increased leaf turnover due to drought stress, but instead are the result of lower leaf production (Nepstad et al., 2002, Schuldt et al., 2011), suggesting
445 an active response of plant allocation strategy to water availability. Concurrently, after 15 years under throughfall exclusion, Rowland et al. (2018) found that leaf litterfall still remained consistently lower. Reported trends in canopy dynamics are therefore in accordance with our findings, and indicate that LAI is a key response mechanism to precipitation regime. Whilst other studies such as da Costa et al.



(2018) have similarly pointed towards structural responses as the principal determinant of variation in
450 GPP, they identify changes in sapwood area as the main driver, rather than LAI. We suggest that whilst
sapwood area may be more important in shaping the response to temporal changes in precipitation, for
forests at steady state, emergent canopy properties (LAI) drive GPP trends.

Photosynthetic capacity also proved an important driver of spatial variation in GPP across the MCWD
gradient. Our results are consistent with a number of Amazon-based studies linking leaf traits to
455 productivity (Aragao et al., 2009, Cleveland et al., 2011, Castanho et al., 2013). Interestingly, the
observed shifts in photosynthetic capacity along the gradient had a compensatory effect on the GPP-
MCWD interaction. Reductions in GPP under high drought stress were alleviated by higher
photosynthetic capacitance. Similarly, shifts in photosynthetic capacity in response to temperature have
been reported to reduce spatial variation in GPP across a tropical elevation gradient (Bahar et al., 2017,
460 van de Weg et al., 2013). Consistent with Fyllas et al. (2017), our results also show that the effect of
climatic forcings on carbon fluxes can be successfully captured through spatial variation in canopy
dynamics and leaf traits. However, as we have focused on the role of leaf traits in the absence of carbon
cycle feedbacks, we do not take into account the effect of concurrent shifts in LMA and leaf lifespan,
which together influence canopy carbon economics (Wright et al., 2004, Osnas et al., 2013, McMurtrie
465 and Dewar, 2011). Furthermore, as nutrient dynamics are not directly accounted for in SPA, we are
unable to quantify the impact of soil nutrients on the GPP-MCWD interaction, beyond its manifestation
in leaf traits. Nevertheless, the interaction between photosynthetic capacity and LAI proved important
in driving variation in GPP across the MCWD gradient.

Root depth, root biomass and soil properties had little direct effect on spatial variation in GPP. Whilst
470 we recognise that the difficulty in measuring root depth and biomass (Metcalf et al., 2007) adds
uncertainty to our results, the findings do not reflect the importance of belowground functioning
highlighted by other studies (Fisher et al., 2007, Metcalfe et al., 2008, Baker et al., 2008, Phillips et al.,
2009, Ichii et al., 2007). Notably, a number of GEM plots had hard pan layers (Quesada et al., 2012) so
may be acclimated to operate in shallow rooting zones, and are therefore not necessarily representative
475 of other Amazon forests under the same precipitation regime. However, it is likely that given these



drivers are largely associated with the acquisition of water, rather than carbon, if feedbacks were enabled within analyses, root and soil properties would prove to have a stronger effect.

4.3 Variation in Forest Sensitivity to Drivers of GPP

The sensitivity of GPP to differences in LAI, climate, photosynthetic capacity and rooting depth varied across the MCWD gradient with evaporative potential and water uptake capacity (Q2; Figure 6). As the model experiment was conducted in the absence of carbon cycle feedbacks, sensitivities reflect shorter rather than long-term effects of changes in forcings. The sensitivity of GPP to differences in LAI and photosynthetic capacity was greatest for forests occupying the lowest drought stress zone and declined with increasing drought stress. Our results are in agreement with findings from Wright et al. (2013), who reported that GPP was most sensitive to decreases in leaf area when water availability was highest. Forests with a high LAI (and therefore high evaporative potential) but shallow rooting depth were most sensitive to differences in climate. Our results suggest that where rooting depth is relatively shallow, and unable to ameliorate the effects of drought stress as seen elsewhere (Nepstad et al., 2007, Malhi et al., 2009a), forests with a high LAI could be more vulnerable to reduced precipitation. Investigations into the vulnerability of Amazon forests to drought have put a deservedly large emphasis on the role of physiological responses (Choat et al., 2012, Phillips et al., 2009, Bennett et al., 2015, Corlett, 2016). However, our results indicate that the role of ecosystem structure could also prove important, and that forests with a high evaporative potential (high LAI) but low water uptake capacity (shallow rooting depth) should be a focus for future studies.

4.4 Drivers of Sub-Annual Variation in GPP

Seasonal variation in GPP was driven by changes in solar radiation, VPD and LAI, the relative importance of which, was dependent on MCWD (Q3; Figure 7). Shortwave radiation was the dominant driver of sub-annual variation in GPP across plots, and its relative effect increased with decreasing drought stress (Table 7). The relative importance of LAI in driving sub-annual GPP increased with drought stress. A number of studies report that for Amazon forests subject to significantly low annual rainfall, GPP declines with increased VPD, and in accordance with our findings, in higher rainfall zones



GPP increases in line with solar radiation (Von Randow et al., 2013, Goulden et al., 2004, Hutyyra et al., 2007, Saleska et al., 2003, Rowland et al., 2014, Carswell et al., 2002). Our results suggest that LAI is not the principal driver of sub-annual variance in GPP, in contrast to its role in driving spatial variation across the MCWD gradient. However, whilst other studies agree that leaf area alone does not drive variation in sub-annual GPP (Wu et al., 2017, Wu et al., 2016, Brando et al., 2010, Restrepo-Coupe et al., 2013, Bi et al., 2015), we fail to account for shifts in photosynthetic capacity with leaf age. The coordination of leaf flushing and new leaf emergence with climatic drivers such as solar radiation is thought to exceed the effects of LAI in non-water limited forests (Myneni et al., 2007). We further recognise the uncertainty introduced through using leaf N content to derive photosynthetic capacity estimates (for five of the seven plots), given the distribution of leaf N between photosynthetic and non-photosynthetic proteins is not fixed (Onoda et al., 2017). However, notwithstanding the effects of temporal variation in photosynthetic capacity, we demonstrate the relative importance of canopy dynamics and climatic forcing driving variation in GPP, shift with light and water availability. Our results indicate that with respect to soil moisture, GPP is demand limited across spatial scales, but is supply limited across sub-annual timescales.

4.5 Limitations and Opportunities

Given the importance of LAI in driving variation in GPP, data on canopy dynamics is critical to constrain carbon flux estimates across the Amazon basin. Our approach utilised field estimates of LAI from hemispherical photographs to constrain model simulations. The accuracy and spatial validity of indirect estimates of LAI has been questioned at higher leaf areas (Bréda, 2003, Jonckheere et al., 2004, Weiss et al., 2004). In this study, we expect that if field measurements of LAI were underestimated at higher leaf areas, the proportion of spatial variation in GPP explained by LAI would increase, as a result of increased variation in both field-measured and model simulated GPP. Yet, our highest estimates of LAI (Caxiuanã $5.11 \pm 1.41 \text{ m}^2\text{m}^{-2}$) align with destructive sampling measurements from a terra-firme Amazon forest (McWilliam et al. (1993) $5.7 \pm 0.5 \text{ m}^2\text{m}^{-2}$). Furthermore, a comparison of LAI estimation approaches (Asner et al., 2003) suggested that indirect methods were appropriate for broadleaved forests, and presented no statistical difference between destructive harvesting and indirect methods.



However, the use of ground measurements is limited to smaller spatial scales, and LAI estimates across
530 the basin are needed to constrain carbon flux estimates. Whilst the interpretation of forest responses to
drought stress through remote sensing approaches have caused controversy (Asner and Alencar, 2010,
Saleska et al., 2007, Samanta et al., 2010), an increase in canopy mapping through satellite missions
could be instrumental to efforts aiming to better understand LAI dynamics. Current and upcoming
satellite missions including FLEX (FLuorescence EXplorer), GEDI (Global Ecosystem Dynamics
535 Investigation) and Sentinel will offer opportunity for new insights into changes in leaves *in-situ*, vertical
canopy structure, and temporal variability via repeat measurements (Morton, 2016, Drusch et al., 2017,
Pettorelli et al., 2018). Efforts to map trait distributions will also prove important (Kattge et al., 2011,
Asner et al., 2015) given their role in driving variation in GPP.

5. Conclusion

540 We show that indirect effects of climate (via ecosystem structure and trait responses) exceed direct
effects (via physiological responses) in driving spatial variation in GPP across an Amazon MCWD
gradient (Q1). Conversely, across sub-annual timescales, the reverse was true (Q3). The relative
sensitivity of GPP to changes in direct and indirect forcings shifted across the MCWD gradient and was
dependent on water availability, demand and acquisition potential (Q2); identifying the potential
545 vulnerability of forests with a high evaporative potential (i.e. high LAI), but low water uptake capacity
(i.e. shallow rooting depth), to changes in precipitation regime. Given the role of LAI in driving GPP
across the drought stress gradient, we highlight a requisite for improved mapping of canopy dynamics
(via remote sensing). We propose that ecosystem model development should focus on the integration
of structural and trait responses to drought stress (alongside physiological responses). The inclusion of
550 both direct and indirect effects of climate in ecosystem models, would reduce current uncertainty in
predicted annual and sub-annual GPP for tropical forests.



555 **Supplementary Material**

Supplementary material is included in a separate document.

Authorship Contributions Sophie Flack-Prain, Mathew Williams and Patrick Meir conceived the research questions. Data used in model calibration and validation was collected by Yadvinder Malhi and associates. Model experiments were designed and conducted by Sophie Flack-Prain with
560 contributions from Mathew Williams and Thomas L. Smallman. Sophie Flack-Prain and Mathew Williams prepared the manuscript with active contributions from all co-authors.

Conflict of Interest Statement: There are no conflicts of interest to disclose.

Acknowledgements: The authors would like to thank the Global Ecosystems Monitoring network team for the field data used in this study, collected through funding from NERC and the Gordon and Betty
565 Moore Foundation, and an ERC Advanced Investigator Award to YM (GEM-TRAIT). The authors would also like to thank the PhD project funding body, the UK Natural Environment Research Council E3 DTP, the National Centre for Earth Observation, the UKSA project Forests 2020 and the Newton CSSP Brazil. The TRY trait database is thanked for the data used in model parameterisation.

570

575



References

- Anderegg, W. R. L.: Spatial and temporal variation in plant hydraulic traits and their relevance for climate change impacts on vegetation, *New Phytologist*, 205(3), 1008-1014, 2015.
- Aragão, L. E. O. C., Malhi, Y., Metcalfe, D. B., Silva-Espejo, J. E., Jimenez, E., Navarrete, D., Almeida, S., Costa, A. C. L., Salinas, N., Phillips, O. L., Anderson, L. O., Alvarez, E., Baker, T. R., Goncalvez, P. H., Huaman-Ovalle, J., Mamani-Solorzano, M., Meir, P., Monteagudo, A., Patino, S., Penuela, M. C., Prieto, A., Quesada, C. A., Rozas-Davila, A., Rudas, A., Silva, J. A., and Vasquez, R.: Above- and below-ground net primary productivity across ten Amazonian forests on contrasting soils, *Biogeosciences*, 6(12), 2759-2778, 2009.
- 585 Aragão, L. E. O. C., Malhi, Y., Roman-Cuesta, R. M., Saatchi, S., Anderson, L. O., and Shimabukuro, Y. E.: Spatial patterns and fire response of recent Amazonian droughts, *Geophysical Research Letters*, 34(7), 2007.
- Araujo-Murakami, A., Doughty, C. E., Metcalfe, D. B., Silva-Espejo, J. E., Arroyo, L., Heredia, J. P., Flores, M., Sibling, R., Mendizabal, L. M., Pardo-Toledo, E., Vega, M., Moreno, L., Rojas-Landivar, V. D., Halladay, K., Girardin, C. A. J., Killeen, T. J., and Malhi, Y.: The productivity, allocation and cycling of carbon in forests at the dry margin of the Amazon forest in Bolivia, *Plant Ecology & Diversity*, 7(1-2), 55-69, 2014.
- Asner, G. P., and Alencar, A.: Drought impacts on the Amazon forest: the remote sensing perspective, *New Phytologist*, 187(3), 569-578, 2010.
- 595 Asner, G. P., Martin, R. E., Anderson, C. B., and Knapp, D. E.: Quantifying forest canopy traits: Imaging spectroscopy versus field survey, *Remote sensing of Environment*, 158, 15-27, 2015.
- Asner, G. P., Scurlock, J. M. O., and Hicke, J. A.: Global synthesis of leaf area index observations: implications for ecological and remote sensing studies, *Global Ecology and Biogeography*, 12(3), 191-205, 2003.



- 600 Bahar, N. H., Ishida, F. Y., Weerasinghe, L. K., Guerrieri, R., O'Sullivan, O. S., Bloomfield, K. J., Asner, G. P., Martin, R. E., Lloyd, J., Malhi, Y., Phillips, O. L., Meir, P., Salinas, N., Cosio, E. G., Domingues, T. F., Quesada, C. A., Sinca, F., Escudero Vega, A., Zuloaga Ccorimanya, P. P., Del Aguila-Pasquel, J., Quispe Huaypar, K., Cuba Torres, I., Butron Loayza, R., Pelaez Tapia, Y., Huaman Ovalle, J., Long, B. M., Evans, J. R., and Atkin, O. K.: Leaf-level photosynthetic capacity in lowland Amazonian and high-elevation Andean tropical moist forests of Peru, *New Phytologist*, 214(3), 1002-1018, 2017.
- Baker, I. T., Prihodko, L., Denning, A. S., Goulden, M., Miller, S., and da Rocha, H. R.: Seasonal drought stress in the Amazon: Reconciling models and observations, *Journal of Geophysical Research-Biogeosciences*, 113(G1), 2008.
- 610 Beer, C., Reichstein, M., Tomelleri, E., Ciais, P., Jung, M., Carvalhais, N., Rodenbeck, C., Arain, M. A., Baldocchi, D., Bonan, G. B., Bondeau, A., Cescatti, A., Lasslop, G., Lindroth, A., Lomas, M., Luysaert, S., Margolis, H., Oleson, K. W., Rouspard, O., Veenendaal, E., Viovy, N., Williams, C., Woodward, F. I., and Papale, D.: Terrestrial gross carbon dioxide uptake: global distribution and covariation with climate, *Science*, 329(5993), 834-838, 2010.
- 615 Bennett, A. C., McDowell, N. G., Allen, C. D., and Anderson-Teixeira, K. J.: Larger trees suffer most during drought in forests worldwide, *Nature Plants*, 1(10), 15139, 2015.
- Bi, J., Knyazikhin, Y., Choi, S. H., Park, T., Barichivich, J., Ciais, P., Fu, R., Ganguly, S., Hall, F., Hilker, T., Huete, A., Jones, M., Kimball, J., Lyapustin, A. I., Mottus, M., Nemani, R. R., Piao, S. L., Poulter, B., Saleska, S. R., Saatchi, S. S., Xu, L., Zhou, L. M., and Myneni, R. B.: Sunlight mediated seasonality in canopy structure and photosynthetic activity of Amazonian rainforests, *Environmental Research Letters*, 10(6), 064014, 2015.
- Bloom, A. A., and Williams, M.: Constraining ecosystem carbon dynamics in a data-limited world: integrating ecological "common sense" in a model-data fusion framework, *Biogeosciences*, 12(5), 1299-1315, 2015.



- 625 Bloom, A. J., Chapin, F. S., and Mooney, H. A.: Resource Limitation in Plants - an Economic Analogy, *Annual review of Ecology and Systematics*, 16, 363-392, 1985.
- Boisier, J. P., Ciais, P., Ducharne, A., and Guimberteau, M.: Projected strengthening of Amazonian dry season by constrained climate model simulations, *Nature Climate Change*, 5(7), 656-660, 2015.
- Bonan, G. B., Williams, M., Fisher, R. A., and Oleson, K. W.: Modeling stomatal conductance in the
630 earth system: linking leaf water-use efficiency and water transport along the soil-plant-atmosphere continuum, *Geoscientific Model Development*, 7(5), 2193-2222, 2014.
- Brando, P. M., Goetz, S. J., Baccini, A., Nepstad, D. C., Beck, P. S., and Christman, M. C.: Seasonal and interannual variability of climate and vegetation indices across the Amazon, *Proceedings of the National Academy of Sciences USA*, 107(33), 14685-14690, 2010.
- 635 Brando, P. M., Nepstad, D. C., Davidson, E. A., Trumbore, S. E., Ray, D., and Camargo, P.: Drought effects on litterfall, wood production and belowground carbon cycling in an Amazon forest: results of a throughfall reduction experiment, *Philosophical Transactions of the Royal Society B: Biological Sciences*, 363(1498), 1839-1848, 2008.
- Bréda, N. J. J.: Ground-based measurements of leaf area index: a review of methods, instruments and
640 current controversies, *Journal of experimental botany*, 54(392), 2403-2417, 2003.
- Breiman, L.: Random forests, *Machine learning*, 45(1), 5-32, 2001.
- Carswell, F. E., Costa, A. L., Palheta, M., Malhi, Y., Meir, P., Costa, J. D. R., Ruivo, M. D., Leal, L. D. M., Costa, J. M. N., Clement, R. J., and Grace, J.: Seasonality in CO₂ and H₂O flux at an eastern Amazonian rain forest, *Journal of Geophysical Research-Atmospheres*, 107(D20), 2002.
- 645 Castanho, A. D. A., Coe, M. T., Costa, M. H., Malhi, Y., Galbraith, D., and Quesada, C. A.: Improving simulated Amazon forest biomass and productivity by including spatial variation in biophysical parameters, *Biogeosciences*, 10(4), 2255-2272, 2013.
- Choat, B., Jansen, S., Brodribb, T. J., Cochard, H., Delzon, S., Bhaskar, R., Bucci, S. J., Feild, T. S., Gleason, S. M., Hacke, U. G., Jacobsen, A. L., Lens, F., Maherali, H., Martinez-Vilalta, J., Mayr, S.,



- 650 Mencuccini, M., Mitchell, P. J., Nardini, A., Pittermann, J., Pratt, R. B., Sperry, J. S., Westoby, M.,
Wright, I. J., and Zanne, A. E.: Global convergence in the vulnerability of forests to drought, *Nature*,
491(7426), 752-755, 2012.
- Cleveland, C. C., Townsend, A. R., Taylor, P., Alvarez-Clare, S., Bustamante, M. M. C., Chuyong,
G., Dobrowski, S. Z., Grierson, P., Harms, K. E., and Houlton, B. Z.: Relationships among net
655 primary productivity, nutrients and climate in tropical rain forest: a pan-tropical analysis, *Ecology*
letters, 14(9), 939-947, 2011.
- Corlett, R. T.: The Impacts of Droughts in Tropical Forests, *Trends Plant Sci*, 21(7), 584-593, 2016.
- da Costa, A. C. L., Rowland, L., Oliveira, R. S., Oliveira, A. A. R., Binks, O. J., Salmon, Y.,
Vasconcelos, S. S., Junior, J. A. S., Ferreira, L. V., Poyatos, R., Mencuccini, M., and Meir, P.: Stand
660 dynamics modulate water cycling and mortality risk in droughted tropical forest, *Global Change*
Biology, 24(1), 249-258, 2018.
- Dee, D. P., Uppala, S. M., Simmons, A. J., Berrisford, P., Poli, P., Kobayashi, S., Andrae, U.,
Balmaseda, M. A., Balsamo, G., and Bauer, P.: The ERA-Interim reanalysis: Configuration and
performance of the data assimilation system, *Quarterly Journal of the royal meteorological society*,
665 137(656), 553-597, 2011.
- Dietze, M. C., Sala, A., Carbone, M. S., Czimczik, C. I., Mantoosh, J. A., Richardson, A. D., and
Vargas, R.: Nonstructural carbon in woody plants, *Annual Review of Plant Biology*, 65, 667-687,
2014.
- Dobbertin, M., Eilmann, B., Bleuler, P., Giuggiola, A., Graf Pannatier, E., Landolt, W., Schleppi, P.,
670 and Rigling, A.: Effect of irrigation on needle morphology, shoot and stem growth in a drought-
exposed *Pinus sylvestris* forest, *Tree Physiology*, 30(3), 346-360, 2010.
- Doughty, C. E., Metcalfe, D. B., Girardin, C. A., Amezquita, F. F., Cabrera, D. G., Huasco, W. H.,
Silva-Espejo, J. E., Araujo-Murakami, A., da Costa, M. C., Rocha, W., Feldpausch, T. R., Mendoza,



- A. L., da Costa, A. C., Meir, P., Phillips, O. L., and Malhi, Y.: Drought impact on forest carbon
675 dynamics and fluxes in Amazonia, *Nature*, 519(7541), 78-82, 2015.
- Drusch, M., Moreno, J., Del Bello, U., Franco, R., Goulas, Y., Huth, A., Kraft, S., Middleton, E. M.,
Miglietta, F., and Mohammed, G.: The FLuorescence EXplorer Mission Concept—ESA’s Earth
Explorer 8, *IEEE Transactions on Geoscience and Remote Sensing*, 55(3), 1273-1284, 2017.
- Duffy, P. B., Brando, P., Asner, G. P., and Field, C. B.: Projections of future meteorological drought
680 and wet periods in the Amazon, *Proceedings of the National Academy of Sciences USA*, 112(43),
13172-13177, 2015.
- Eller, C. B., Rowland, L., Oliveira, R. S., Bittencourt, P. R. L., Barros, F. V., da Costa, A. C. L., Meir,
P., Friend, A. D., Mencuccini, M., Sitch, S., and Cox, P.: Modelling tropical forest responses to
drought and El Nino with a stomatal optimization model based on xylem hydraulics, *Philosophical*
685 *Transactions of the Royal Society B: Biological Sciences*, 373(1760), 20170315, 2018.
- Food and Agriculture Organization (FAO): World Reference Base for Soil Resources 2014
International Soil Classification System for Naming Soils and Creating Legends for Soil Maps, FAO:
Rome, 2014.
- Fauset, S., Baker, T. R., Lewis, S. L., Feldpausch, T. R., Affum-Baffoe, K., Foli, E. G., Hamer, K. C.,
690 and Swaine, M. D.: Drought-induced shifts in the floristic and functional composition of tropical
forests in Ghana, *Ecology Letters*, 15(10), 1120-1129, 2012.
- Fisher, R. A., Koven, C. D., Anderegg, W. R. L., Christoffersen, B. O., Dietze, M. C., Farrior, C. E.,
Holm, J. A., Hurtt, G. C., Knox, R. G., Lawrence, P. J., Lichstein, J. W., Longo, M., Matheny, A. M.,
Medvigy, D., Muller-Landau, H. C., Powell, T. L., Serbin, S. P., Sato, H., Shuman, J. K., Smith, B.,
695 Trugman, A. T., Viskari, T., Verbeeck, H., Weng, E., Xu, C., Xu, X., Zhang, T., and Moorcroft, P. R.:
Vegetation demographics in Earth System Models: A review of progress and priorities, *Global*
Change Biology, 24(1), 35-54, 2018.



- Fisher, R. A., Williams, M., Da Costa, A. L., Malhi, Y., Da Costa, R. F., Almeida, S., and Meir, P.:
The response of an Eastern Amazonian rain forest to drought stress: results and modelling analyses
700 from a throughfall exclusion experiment, *Global Change Biology*, 13(11), 2361-2378, 2007.
- Fisher, R. A., Williams, M., Do Vale, R. L., Da Costa, A. L., and Meir, P.: Evidence from Amazonian
forests is consistent with isohydric control of leaf water potential, *Plant Cell and Environment*, 29(2),
151-165, 2006.
- Fyllas, N. M., Bentley, L. P., Shenkin, A., Asner, G. P., Atkin, O. K., Diaz, S., Enquist, B. J., Farfan-
705 Rios, W., Gloor, E., Guerrieri, R., Huasco, W. H., Ishida, Y., Martin, R. E., Meir, P., Phillips, O.,
Salinas, N., Silman, M., Weerasinghe, L. K., Zaragoza-Castells, J., and Malhi, Y.: Solar radiation and
functional traits explain the decline of forest primary productivity along a tropical elevation gradient,
Ecology Letters, 20(6), 730-740, 2017.
- Fyllas, N. M., Patino, S., Baker, T. R., Bielefeld Nardoto, G., Martinelli, L. A., Quesada, C. A., Paiva,
710 R., Schwarz, M., Horna, V., and Mercado, L. M.: Basin-wide variations in foliar properties of
Amazonian forest: phylogeny, soils and climate, *Biogeosciences*, 6, 2677-2708, 2009.
- Galbraith, D., Levy, P. E., Sitch, S., Huntingford, C., Cox, P., Williams, M., and Meir, P.: Multiple
mechanisms of Amazonian forest biomass losses in three dynamic global vegetation models under
climate change, *New Phytologist*, 187(3), 647-665, 2010.
- 715 Goulden, M. L., Miller, S. D., da Rocha, H. R., Menton, M. C., de Freitas, H. C., Figueira, A. M. E.
S., and de Sousa, C. A. D.: Diel and seasonal patterns of tropical forest CO₂ exchange, *Ecological
Applications*, 14(4), S42-S54, 2004.
- Green, J. K., Seneviratne, S. I., Berg, A. M., Findell, K. L., Hagemann, S., Lawrence, D. M., and
Gentine, P.: Large influence of soil moisture on long-term terrestrial carbon uptake, *Nature*, 565, 476-
720 479, 2019.
- Grier, C. C., and Running, S. W.: Leaf Area of Mature Northwestern Coniferous Forests - Relation to
Site Water-Balance, *Ecology*, 58(4), 893-899, 1977.



- Hutyra, L. R., Munger, J. W., Saleska, S. R., Gottlieb, E., Daube, B. C., Dunn, A. L., Amaral, D. F., De Camargo, P. B., and Wofsy, S. C.: Seasonal controls on the exchange of carbon and water in an Amazonian rain forest, *Journal of Geophysical Research: Biogeosciences*, 112(G3), 2007.
- 725
- Ichii, K., Hashimoto, H., White, M. A., Potters, C., Hutyra, L. R., Huete, A. R., Myneni, R. B., and Nemanis, R. R.: Constraining rooting depths in tropical rainforests using satellite data and ecosystem modeling for accurate simulation of gross primary production seasonality, *Global Change Biology*, 13(1), 67-77, 2007.
- 730
- Iio, A., Hikosaka, K., Anten, N. P. R., Nakagawa, Y., and Ito, A.: Global dependence of field-observed leaf area index in woody species on climate: a systematic review, *Global Ecology and Biogeography*, 23(3), 274-285, 2014.
- Joetzjer, E., Douville, H., Delire, C., and Ciais, P.: Present-day and future Amazonian precipitation in global climate models: CMIP5 versus CMIP3, *Climate Dynamics*, 41(11-12), 2921-2936, 2013.
- 735
- Jonckheere, I., Fleck, S., Nackaerts, K., Muys, B., Coppin, P., Weiss, M., and Baret, F.: Review of methods for in situ leaf area index determination - Part I. Theories, sensors and hemispherical photography, *Agricultural and Forest Meteorology*, 121(1-2), 19-35, 2004.
- Kattge, J., Diaz, S., Lavorel, S., Prentice, I. C., Leadley, P., Bönsch, G., Garnier, E., Westoby, M., Reich, P. B., and Wright, I. J.: TRY—a global database of plant traits, *Global Change Biology*, 17(9), 2905-2935, 2011.
- 740
- Lee, J. E., Frankenberg, C., van der Tol, C., Berry, J. A., Guanter, L., Boyce, C. K., Fisher, J. B., Morrow, E., Worden, J. R., Asefi, S., Badgley, G., and Saatchi, S.: Forest productivity and water stress in Amazonia: observations from GOSAT chlorophyll fluorescence, *Proceedings of the Royal Society B: Biological Sciences*, 280(1761), 20130171, 2013.
- 745
- Liu, J., Bowman, K. W., Schimel, D. S., Parazoo, N. C., Jiang, Z., Lee, M., Bloom, A. A., Wunch, D., Frankenberg, C., and Sun, Y.: Contrasting carbon cycle responses of the tropical continents to the 2015–2016 El Niño, *Science*, 358(6360), eaam5690, 2017.



López-Blanco, E., Lund, M., Williams, M., Tamstorf, M. P., Westergaard-Nielsen, A., Exbrayat, J.-F., Hansen, B. U., and Christensen, T. R.: Exchange of CO₂ in Arctic tundra: impacts of meteorological variations and biological disturbance, *Biogeosciences*, 14(19), 4467-4483, 2017.

Malhi, Y., Amezquita, F. F., Doughty, C. E., Silva-Espejo, J. E., Girardin, C. A. J., Metcalfe, D. B., Aragão, L. E. O. C., Huaraca-Quispe, L. P., Alzamora-Taype, I., Eguiluz-Mora, L., Marthews, T. R., Halladay, K., Quesada, C. A., Robertson, A. L., Fisher, J. B., Zaragoza-Castells, J., Rojas-Villagra, C. M., Pelaez-Tapia, Y., Salinas, N., Meir, P., and Phillips, O. L.: The productivity, metabolism and carbon cycle of two lowland tropical forest plots in south-western Amazonia, Peru, *Plant Ecology & Diversity*, 7(1-2), 85-105, 2014.

Malhi, Y., Aragão, L. E., Galbraith, D., Huntingford, C., Fisher, R., Zelazowski, P., Sitch, S., McSweeney, C., and Meir, P.: Exploring the likelihood and mechanism of a climate-change-induced dieback of the Amazon rainforest, *Proceedings of the National Academy of Sciences*, 106(49), 20610-20615, 2009.

Malhi, Y., Doughty, C. E., Goldsmith, G. R., Metcalfe, D. B., Girardin, C. A. J., Marthews, T. R., del Aguila-Pasquel, J., Aragão, L. E. O. C., Araujo-Murakami, A., Brando, P., da Costa, A. C. L., Silva-Espejo, J. E., Amezquita, F. F., Galbraith, D. R., Quesada, C. A., Rocha, W., Salinas-Revilla, N., Silverio, D., Meir, P., and Phillips, O. L.: The linkages between GPP, productivity, growth and biomass in lowland Amazonian forests, *Global Change Biology*, 21(6), 2283-2295, 2015.

Malhi, Y., Roberts, J. T., Betts, R. A., Killeen, T. J., Li, W., and Nobre, C. A.: Climate change, deforestation, and the fate of the Amazon, *Science*, 319(5860), 169-172, 2008.

McMurtrie, R. E., and Dewar, R. C.: Leaf-trait variation explained by the hypothesis that plants maximize their canopy carbon export over the lifespan of leaves, *Tree Physiology*, 31(9), 1007-1023, 2011.

McWilliam, A. L., Roberts, J. M., Cabral, O. M. R., Leitao, M., De Costa, A. C. L., Maitelli, G. T., and Zamparoni, C.: Leaf area index and above-ground biomass of terra firme rain forest and adjacent clearings in Amazonia, *Functional ecology*, 310-317, 1993.



- Meir, P., Brando, P. M., Nepstad, D., Vasconcelos, S., Costa, A. C. L., Davidson, E., Almeida, S.,
775 Fisher, R. A., Sotta, E. D., Zarin, D., and Cardinot, G.: The Effects of Drought on Amazonian Rain
Forests, *Amazonia and Global Change*, 186, 429-449, 2009.
- Meir, P., Mencuccini, M., and Dewar, R. C.: Drought-related tree mortality: addressing the gaps in
understanding and prediction, *New Phytologist*, 207(1), 28-33, 2015b.
- Meir, P., Metcalfe, D. B., Costa, A. C., and Fisher, R. A.: The fate of assimilated carbon during
780 drought: impacts on respiration in Amazon rainforests, *Philosophical Transactions of the Royal
Society B: Biological Sciences*, 363(1498), 1849-1855, 2008.
- Meir, P., Wood, T. E., Galbraith, D. R., Brando, P. M., Da Costa, A. C., Rowland, L., and Ferreira, L.
V.: Threshold Responses to Soil Moisture Deficit by Trees and Soil in Tropical Rain Forests: Insights
from Field Experiments, *Bioscience*, 65(9), 882-892, 2015a.
- 785 Meir, P., and Woodward, F. I.: Amazonian rain forests and drought: response and vulnerability, *New
Phytologist*, 187(3), 553-557, 2010.
- Mercado, L. M., Patino, S., Domingues, T. F., Fyllas, N. M., Weedon, G. P., Sitch, S., Quesada, C.
A., Phillips, O. L., Aragão, L. E., Malhi, Y., Dolman, A. J., Restrepo-Coupe, N., Saleska, S. R.,
Baker, T. R., Almeida, S., Higuchi, N., and Lloyd, J.: Variations in Amazon forest productivity
790 correlated with foliar nutrients and modelled rates of photosynthetic carbon supply, *Philosophical
Transactions of the Royal Society B: Biological Sciences*, 366(1582), 3316-3329, 2011.
- Metcalfe, D. B., Meir, P., Aragão, L., Malhi, Y., Da Costa, A. C. L., Braga, A., Gonçalves, P. H. L.,
de Athaydes, J., De Almeida, S. S., and Williams, M.: Factors controlling spatio-temporal variation in
carbon dioxide efflux from surface litter, roots, and soil organic matter at four rain forest sites in the
795 eastern Amazon, *Journal of Geophysical Research: Biogeosciences*, 112(G4), 2007.
- Metcalfe, D. B., Meir, P., Aragão, L. E. O. C., da Costa, A. C. L., Braga, A. P., Gonçalves, P. H. L.,
Silva, J. D., de Almeida, S. S., Dawson, L. A., Malhi, Y., and Williams, M.: The effects of water



- availability on root growth and morphology in an Amazon rainforest, *Plant and Soil*, 311(1-2), 189-199, 2008.
- 800 Metcalfe, D. B., Meir, P., Aragão, L. E. O. C., Lobo-do-Vale, R., Galbraith, D., Fisher, R. A., Chaves, M. M., Maroco, J. P., da Costa, A. C. L., and de Almeida, S. S.: Shifts in plant respiration and carbon use efficiency at a large-scale drought experiment in the eastern Amazon, *New Phytologist*, 187(3), 608-621, 2010.
- Moore, C. E., Beringer, J., Donohue, R. J., Evans, B., Exbrayat, J. F., Hutley, L. B., and Tapper, N. J.:
805 Seasonal, interannual and decadal drivers of tree and grass productivity in an Australian tropical savannah, *Global Change Biology*, 24(6), 2530-2544, 2018.
- Morton, D. C.: FOREST CARBON FLUXES A satellite perspective, *Nature Climate Change*, 6(4), 346-348, 2016.
- Myneni, R. B., Yang, W., Nemani, R. R., Huete, A. R., Dickinson, R. E., Knyazikhin, Y., Didan, K.,
810 Fu, R., Negron Juarez, R. I., Saatchi, S. S., Hashimoto, H., Ichii, K., Shabanov, N. V., Tan, B., Ratana, P., Privette, J. L., Morisette, J. T., Vermote, E. F., Roy, D. P., Wolfe, R. E., Friedl, M. A., Running, S. W., Votava, P., El-Saleous, N., Devadiga, S., Su, Y., and Salomonson, V. V.: Large seasonal swings in leaf area of Amazon rainforests, *Proceedings of the National Academy of Sciences*, 104(12), 4820-4823, 2007.
- 815 Nepstad, D. C., Decarvalho, C. R., Davidson, E. A., Jipp, P. H., Lefebvre, P. A., Negreiros, G. H., Dasilva, E. D., Stone, T. A., Trumbore, S. E., and Vieira, S.: The Role of Deep Roots in the Hydrological and Carbon Cycles of Amazonian Forests and Pastures, *Nature*, 372(6507), 666-669, 1994.
- Nepstad, D. C., Moutinho, P., Dias, M. B., Davidson, E., Cardinot, G., Markewitz, D., Figueiredo, R.,
820 Vianna, N., Chambers, J., Ray, D., Guerreiros, J. B., Lefebvre, P., Sternberg, L., Moreira, M., Barros, L., Ishida, F. Y., Tohlver, I., Belk, E., Kalif, K., and Schwalbe, K.: The effects of partial throughfall exclusion on canopy processes, aboveground production, and biogeochemistry of an Amazon forest, *Journal of Geophysical Research-Atmospheres*, 107(D20), 2002.



- Nepstad, D. C., Tohver, I. M., Ray, D., Moutinho, P., and Cardinot, G.: Mortality of large trees and
825 lianas following experimental drought in an Amazon forest, *Ecology*, 88(9), 2259-2269, 2007.
- Onoda, Y., Wright, I. J., Evans, J. R., Hikosaka, K., Kitajima, K., Niinemets, Ü., Poorter, H., Tosens,
T., and Westoby, M.: Physiological and structural tradeoffs underlying the leaf economics spectrum,
New Phytologist, 214(4), 1447-1463, 2017.
- Osnas, J. L., Lichstein, J. W., Reich, P. B., and Pacala, S. W.: Global leaf trait relationships: mass,
830 area, and the leaf economics spectrum, *Science*, 340(6133), 741-744, 2013.
- Pedregosa, F., Varoquaux, G., Gramfort, A., Michel, V., Thirion, B., Grisel, O., Blondel, M.,
Prettenhofer, P., Weiss, R., Dubourg, V., Vanderplas, J., Passos, A., Cournapeau, D., Brucher, M.,
Perrot, M., and Duchesnay, E.: Scikit-learn: Machine Learning in Python, *Journal of machine learning
research*, 12(Oct), 2825-2830, 2011.
- 835 Pettorelli, N., Buhne, H. S. T., Tulloch, A., Dubois, G., Macinnis-Ng, C., Queiros, A. M., Keith, D.
A., Wegmann, M., Schrod, F., Stellmes, M., Sonnenschein, R., Geller, G. N., Roy, S., Somers, B.,
Murray, N., Bland, L., Geijzendorffer, I., Kerr, J. T., Broszeit, S., Leitao, P. J., Duncan, C., El Serafy,
G., He, K. S., Blanchard, J. L., Lucas, R., Mairota, P., Webb, T. J., and Nicholson, E.: Satellite remote
sensing of ecosystem functions: opportunities, challenges and way forward, *Remote Sensing in
840 Ecology and Conservation*, 4(2), 71-93, 2018.
- Phillips, O. L., Aragão, L. E., Lewis, S. L., Fisher, J. B., Lloyd, J., Lopez-Gonzalez, G., Malhi, Y.,
Monteagudo, A., Peacock, J., Quesada, C. A., van der Heijden, G., Almeida, S., Amaral, I., Arroyo,
L., Aymard, G., Baker, T. R., Banki, O., Blanc, L., Bonal, D., Brando, P., Chave, J., de Oliveira, A.
C., Cardozo, N. D., Czimeczik, C. I., Feldpausch, T. R., Freitas, M. A., Gloor, E., Higuchi, N.,
845 Jimenez, E., Lloyd, G., Meir, P., Mendoza, C., Morel, A., Neill, D. A., Nepstad, D., Patino, S.,
Penuela, M. C., Prieto, A., Ramirez, F., Schwarz, M., Silva, J., Silveira, M., Thomas, A. S., Steege, H.
T., Stropp, J., Vasquez, R., Zelazowski, P., Alvarez Davila, E., Andelman, S., Andrade, A., Chao, K.
J., Erwin, T., Di Fiore, A., Honorio, C. E., Keeling, H., Killeen, T. J., Laurance, W. F., Pena Cruz, A.,
Pitman, N. C., Nunez Vargas, P., Ramirez-Angulo, H., Rudas, A., Salamao, R., Silva, N., Terborgh,



- 850 J., and Torres-Lezama, A.: Drought sensitivity of the Amazon rainforest, *Science*, 323(5919), 1344-1347, 2009.
- Poorter, L. and Bongers, F.: Leaf traits are good predictors of plant performance across 53 rain forest species, *Ecology*, 87, 1733-1743, 2006.
- Powell, T. L., Galbraith, D. R., Christoffersen, B. O., Harper, A., Imbuzeiro, H. M., Rowland, L., Almeida, S., Brando, P. M., da Costa, A. C., Costa, M. H., Levine, N. M., Malhi, Y., Saleska, S. R., Sotta, E., Williams, M., Meir, P., and Moorcroft, P. R.: Confronting model predictions of carbon fluxes with measurements of Amazon forests subjected to experimental drought, *New Phytologist*, 200(2), 350-365, 2013.
- 860 Quesada, C. A., Phillips, O. L., Schwarz, M., Czimczik, C. I., Baker, T. R., Patino, S., Fyllas, N. M., Hodnett, M. G., Herrera, R., Almeida, S., Davila, E. A., Arneeth, A., Arroyo, L., Chao, K. J., Dezzeeo, N., Erwin, T., di Fiore, A., Higuchi, N., Coronado, E. H., Jimenez, E. M., Killeen, T., Lezama, A. T., Lloyd, G., Lopez-Gonzalez, G., Luizao, F. J., Malhi, Y., Monteagudo, A., Neill, D. A., Vargas, P. N., Paiva, R., Peacock, J., Penuela, M. C., Cruz, A. P., Pitman, N., Priante, N., Prieto, A., Ramirez, H., Rudas, A., Salomao, R., Santos, A. J. B., Schmerler, J., Silva, N., Silveira, M., Vasquez, R., Vieira, I.,
- 865 Terborgh, J., and Lloyd, J.: Basin-wide variations in Amazon forest structure and function are mediated by both soils and climate, *Biogeosciences*, 9(6), 2203-2246, 2012.
- Reich, P. B., Tjoelker, M. G., Pregitzer, K. S., Wright, I. J., Oleksyn, J., and Machado, J. L.: Scaling of respiration to nitrogen in leaves, stems and roots of higher land plants, *Ecology Letters*, 11(8), 793-801, 2008.
- 870 Reich, P. B., Uhl, C., Walters, M. B., and Ellsworth, D. S.: Leaf lifespan as a determinant of leaf structure and function among 23 Amazonian tree species, *Oecologia*, 86(1), 16-24, 1991.
- Reichstein, M., Bahn, M., Mahecha, M. D., Kattge, J., and Baldocchi, D. D.: Linking plant and ecosystem functional biogeography, *Proceedings of the National Academy of Sciences*, 111(38), 13697-13702, 2014.



- 875 Restrepo-Coupe, N., da Rocha, H. R., Hutrya, L. R., da Araujo, A. C., Borma, L. S., Christoffersen, B., Cabral, O. M. R., de Camargo, P. B., Cardoso, F. L., and da Costa, A. C. L.: What drives the seasonality of GPP across the Amazon basin? A cross-site analysis of eddy flux tower measurements from the Brasil flux network, *Agricultural and Forest Meteorology*, 182, 128-144, 2013.
- Restrepo-Coupe, N., Levine, N. M., Christoffersen, B. O., Albert, L. P., Wu, J., Costa, M. H.,
- 880 Galbraith, D., Imbuzeiro, H., Martins, G., and Araujo, A. C.: Do dynamic global vegetation models capture the seasonality of carbon fluxes in the Amazon basin? A data-model intercomparison, *Global Change Biology*, 23(1), 191-208, 2017.
- Rocha, W., Metcalfe, D. B., Doughty, C. E., Brando, P., Silverio, D., Halladay, K., Nepstad, D. C., Balch, J. K., and Malhi, Y.: Ecosystem productivity and carbon cycling in intact and annually burnt
- 885 forest at the dry southern limit of the Amazon rainforest (Mato Grosso, Brazil), *Plant Ecology & Diversity*, 7(1-2), 25-40, 2014.
- Rodig, E., Cuntz, M., Rammig, A., Fischer, R., Taubert, F., and Huth, A.: The importance of forest structure for carbon fluxes of the Amazon rainforest, *Environmental Research Letters*, 13(5), 054013, 2018.
- 890 Rowland, L., Da Costa, A. C. L., Galbraith, D. R., Oliveira, R. S., Binks, O. J., Oliveira, A. A. R., Pullen, A. M., Doughty, C. E., Metcalfe, D. B., and Vasconcelos, S. S.: Death from drought in tropical forests is triggered by hydraulics not carbon starvation, *Nature*, 528(7580), 119-122, 2015a.
- Rowland, L., da Costa, A. C. L., Oliveira, A. A. R., Almeida, S. S., Ferreira, L. V., Malhi, Y., Metcalfe, D. B., Mencuccini, M., Grace, J., and Meir, P.: Shock and stabilisation following long-term
- 895 drought in tropical forest from 15 years of litterfall dynamics, *Journal of ecology*, 106(4), 1673-1682, 2018.
- Rowland, L., Harper, A., Christoffersen, B. O., Galbraith, D. R., Imbuzeiro, H. M. A., Powell, T. L., Doughty, C., Levine, N. M., Malhi, Y., Saleska, S. R., Moorcroft, P. R., Meir, P., and Williams, M.: Modelling climate change responses in tropical forests: similar productivity estimates across five



- 900 models, but different mechanisms and responses, *Geoscientific Model Development*, 8(4), 1097-1110, 2015b.
- Rowland, L., Hill, T. C., Stahl, C., Siebicke, L., Burban, B., Zaragoza-Castells, J., Ponton, S., Bonal, D., Meir, P., and Williams, M.: Evidence for strong seasonality in the carbon storage and carbon use efficiency of an Amazonian forest, *Global Change Biology*, 20(3), 979-991, 2014.
- 905 Sakschewski, B., von Bloh, W., Boit, A., Poorter, L., Pena-Claros, M., Heinke, J., Joshi, J., and Thonicke, K.: Resilience of Amazon forests emerges from plant trait diversity, *Nature Climate Change*, 6(11), 1032-1036, 2016.
- Saleska, S. R., Didan, K., Huete, A. R., and da Rocha, H. R.: Amazon forests green-up during 2005 drought, *Science*, 318(5850), 612, 2007.
- 910 Saleska, S. R., Miller, S. D., Matross, D. M., Goulden, M. L., Wofsy, S. C., da Rocha, H. R., de Camargo, P. B., Crill, P., Daube, B. C., de Freitas, H. C., Hutyrá, L., Keller, M., Kirchhoff, V., Menton, M., Munger, J. W., Pyle, E. H., Rice, A. H., and Silva, H.: Carbon in Amazon forests: unexpected seasonal fluxes and disturbance-induced losses, *Science*, 302(5650), 1554-1557, 2003.
- Samanta, A., Ganguly, S., Hashimoto, H., Devadiga, S., Vermote, E., Knyazikhin, Y., Nemani, R. R., 915 and Myneni, R. B.: Amazon forests did not green-up during the 2005 drought, *Geophysical Research Letters*, 37(5), 2010.
- Santiago, L. S., Kitajima, K., Wright, S. J., and Mulkey, S. S.: Coordinated changes in GPP, water relations and leaf nutritional traits of canopy trees along a precipitation gradient in lowland tropical forest, *Oecologia*, 139(4), 495-502, 2004.
- 920 Saxton, K. E., Rawls, W. J., Romberger, J. S., and Papendick, R. I.: Estimating generalized soil-water characteristics from texture 1, *Soil Science Society of America Journal*, 50(4), 1031-1036, 1986.
- Schleppi, P., Thimonier, A., and Walthert, L.: Estimating leaf area index of mature temperate forests using regressions on site and vegetation data, *Forest Ecology and Management*, 261(3), 601-610, 2011.



- 925 Schuldt, B., Leuschner, C., Horna, V., Moser, G., Koler, M., van Straaten, O., and Barus, H.: Change in hydraulic properties and leaf traits in a tall rainforest tree species subjected to long-term throughfall exclusion in the perhumid tropics, *Biogeosciences*, 8(8), 2179-2194, 2011.
- Smallman, T. L., Moncrieff, J. B., and Williams, M.: WRFv3. 2-SPAv2: development and validation of a coupled ecosystem–atmosphere model, scaling from surface fluxes of CO₂ and energy to
930 atmospheric profiles, *Geoscientific Model Development*, 6(4), 1079-1093, 2013.
- Sperry, J. S., Hacke, U. G., Oren, R., and Comstock, J. P.: Water deficits and hydraulic limits to leaf water supply, *Plant Cell and Environment*, 25(2), 251-263, 2002.
- van de Weg, M. J., Shaver, G. R., and Salmon, V. G.: Contrasting effects of long term versus short-term nitrogen addition on GPP and respiration in the Arctic, *Plant Ecology*, 214(10), 1273-1286,
935 2013.
- Von Randow, C., Zeri, M., Restrepo-Coupe, N., Muza, M. N., de Gonçalves, L. G. G., Costa, M. H., Araujo, A. C., Manzi, A. O., da Rocha, H. R., and Saleska, S. R.: Inter-annual variability of carbon and water fluxes in Amazonian forest, Cerrado and pasture sites, as simulated by terrestrial biosphere models, *Agricultural and Forest Meteorology*, 182, 145-155, 2013.
- 940 Wagner, F. H., Herault, B., Rossi, V., Hilker, T., Maeda, E. E., Sanchez, A., Lyapustin, A. I., Galvao, L. S., Wang, Y., and Aragão, L.: Climate drivers of the Amazon forest greening, *PloS one*, 12(7), e0180932, 2017.
- Walker, A. P., Beckerman, A. P., Gu, L., Kattge, J., Cernusak, L. A., Domingues, T. F., Scales, J. C., Wohlfahrt, G., Wullschlegel, S. D., and Woodward, F. I.: The relationship of leaf photosynthetic
945 traits–V_{cmax} and J_{max}–to leaf nitrogen, leaf phosphorus, and specific leaf area: a meta-analysis and modeling study, *Ecology and evolution*, 4, 3218-3235, 2014.
- Waring, R. H., and Schlesinger, W. H.: *Forest ecosystems, Concepts and management*: Academic Press. Orlando, FL, 1985.



- Weiss, M., Baret, F., Smith, G. J., Jonckheere, I., and Coppin, P.: Review of methods for in situ leaf area index (LAI) determination Part II. Estimation of LAI, errors and sampling, *Agricultural and Forest Meteorology*, 121(1-2), 37-53, 2004.
- Williams, M., Malhi, Y., Nobre, A. D., Rastetter, E. B., Grace, J., and Pereira, M. G. P.: Seasonal variation in net carbon exchange and evapotranspiration in a Brazilian rain forest: a modelling analysis, *Plant Cell and Environment*, 21(10), 953-968, 1998.
- 955 Williams, M., Rastetter, E. B., Fernandes, D. N., Goulden, M. L., Wofsy, S. C., Shaver, G. R., Melillo, J. M., Munger, J. W., Fan, S. M., and Nadelhoffer, K. J.: Modelling the soil-plant-atmosphere continuum in a *Quercus*–*Acer* stand at Harvard Forest: the regulation of stomatal conductance by light, nitrogen and soil/plant hydraulic properties, *Plant, Cell and Environment*, 19(8), 911-927, 1996.
- 960 Wright, I. J., Reich, P. B., Westoby, M., Ackerly, D. D., Baruch, Z., Bongers, F., Cavender-Bares, J., Chapin, T., Cornelissen, J. H., Diemer, M., Flexas, J., Garnier, E., Groom, P. K., Gulias, J., Hikosaka, K., Lamont, B. B., Lee, T., Lee, W., Lusk, C., Midgley, J. J., Navas, M. L., Niinemets, U., Oleksyn, J., Osada, N., Poorter, H., Poot, P., Prior, L., Pyankov, V. I., Roumet, C., Thomas, S. C., Tjoelker, M. G., Veneklaas, E. J., and Villar, R.: The worldwide leaf economics spectrum, *Nature*, 428(6985), 821-827, 2004.
- 965 Wright, J. K., Williams, M., Starr, G., McGee, J., and Mitchell, R. J.: Measured and modelled leaf and stand-scale productivity across a soil moisture gradient and a severe drought, *Plant Cell and Environment*, 36(2), 467-483, 2013.
- Wu, J., Albert, L. P., Lopes, A. P., Restrepo-Coupe, N., Hayek, M., Wiedemann, K. T., Guan, K., Stark, S. C., Christoffersen, B., Prohaska, N., Tavares, J. V., Marostica, S., Kobayashi, H., Ferreira, M. L., Campos, K. S., da Silva, R., Brando, P. M., Dye, D. G., Huxman, T. E., Huete, A. R., Nelson, B. W., and Saleska, S. R.: Leaf development and demography explain photosynthetic seasonality in Amazon evergreen forests, *Science*, 351(6276), 972-976, 2016.
- Wu, J., Guan, K. Y., Hayek, M., Restrepo-Coupe, N., Wiedemann, K. T., Xu, X. T., Wehr, R., Christoffersen, B. O., Miao, G. F., da Silva, R., de Araujo, A. C., Oliviera, R. C., Camargo, P. B.,



975 Monson, R. K., Huete, A. R., and Saleska, S. R.: Partitioning controls on Amazon forest GPP between environmental and biotic factors at hourly to interannual timescales, *Global Change Biology*, 23(3), 1240-1257, 2017.

Zhang, K., Castanho, A. D. D., Galbraith, D. R., Moghim, S., Levine, N. M., Bras, R. L., Coe, M. T., Costa, M. H., Malhi, Y., Longo, M., Knox, R. G., McKnight, S., Wang, J. F., and Moorcroft, P. R.:

980 The fate of Amazonian ecosystems over the coming century arising from changes in climate, atmospheric CO₂, and land use, *Global Change Biology*, 21(7), 2569-2587, 2015.

985

990



995 Tables

Table 1. Environmental characteristics of GEM network Amazon permanent sample plots across the MCWD gradient. Meteorological data is from local weather stations, gap filled with ERA interim data for the years 2009-2010 (Dee et al., 2011).

Plot name	Caxiuanã	Caxiuanã	Tambopata	Tambopata	Kenia	Kenia	Tanguro
	Control	Tower	V	VI	Wet	Dry	Control
RAINFOR	CAX04	CAX06	TAM05	TAM06	KEN01	KEN02	---
site code							
Latitude	-1.716	-1.737	-12.831	-12.839	-16.016	-16.016	-13.077
Longitude	-51.457	-51.462	-69.271	-69.296	-62.73	-62.73	-52.386
Elevation (m.a.s.l)	47		223		384		385
Mean Maximum Climatological Water Deficit (mm)	-85.5		-256		-342		-498
Mean annual air temperature (°C)	26.1		24.6		23.4		25.4
Soil Type	Vetic Acrisol	Ferralsol	Cambisol	Alisol	Cambisol	Cambisol	Ferralsol
Soil N (%)	0.06	0.13	0.16	0.17	0.22	0.17	0.16
Soil P _{total} (mg kg ⁻¹)	37.4	178.5	256.3	528.8	447.1	244.7	147



1005 Table 2. Summary of the relationship between model variables and field data. Values are either a SPA model parameter (input) or output. Model parameters may be initial conditions subsequently allowed to fluctuate, a fixed value, or a time-series, whereby the parameter value at each time point is prescribed to the model. Model outputs are generated on either an hourly or daily time-step and are presented in the text as the mean annual sum (2009-2010), unless otherwise stated. Model outputs are calibrated or evaluated using field data. Values are specific to each of the seven GEM Amazonian permanent sample plots.

Value	Model Parameter or Output	Source of Value or Calibration/Validation Data
LMA	parameter (single fixed)	GEM plot-measured value or literature-based estimate from plot species list
V_{max}	parameter (single fixed)	(estimate from) GEM plot-measured value or TRY database estimate from plot species list
J_{max}	parameter (single fixed)	(estimate from) GEM plot-measured value or TRY database estimate from plot species list
Leaf N content	parameter (single fixed)	GEM plot-measured value or TRY database estimate from plot species list
LAI	parameter (timeseries fixed)	GEM monthly plot-measured value
Leaf NPP	output	model calibration to GEM plot-measured leaf litterfall and LAI
Wood NPP		



<i>fraction of total NPP</i>	parameter (single fixed)	GEM plot-measured value
<i>total wood NPP</i>	output	simulated value validated against GEM field-measured total wood NPP
Root NPP		
<i>fraction of total NPP</i>	parameter (single fixed)	GEM plot-measured value
<i>total root NPP</i>	output	simulated value validated against GEM field-measured total root NPP
Leaf turnover	parameter (single fixed; function of three individual parameters relating to the litterfall cycle)	model calibration to GEM plot-measured leaf litterfall
Root turnover	parameter (single fixed)	estimated using root NPP assuming steady state conditions
Wood turnover	parameter (single fixed)	estimated using wood NPP assuming steady state conditions
Foliar C stock	parameter (timeseries fixed)	product of LAI and LMA



Wood C stock	parameter	initial	condition;	initial condition uses GEM plot-measured DBH values converted to C stock using allometric equation output calculated in SPA as simulated wood C stock plus NPP minus turnover
	thereafter	output		
Root C stock	parameter	initial	condition;	initial condition used GEM plot-measured root stock values or literature-based estimate output calculated in SPA as simulated root C stock plus NPP minus turnover
	thereafter	output		
Leaf respiration	output			sum of leaf maintenance and growth respiration; maintenance respiration generated using measured leaf N content, foliar C stock and the Reich <i>et al.</i> , (2008) leaf respiration model, validated against GEM estimates; growth respiration calculated in SPA as leaf NPP \times 0.28
Wood respiration	output			sum of wood maintenance and growth respiration; maintenance respiration calculated as a function of wood C stock, the coefficient being derived from GEM estimates; growth respiration calculated in SPA as wood NPP \times 0.28
Root respiration	output			sum of root maintenance and growth respiration; maintenance respiration calculated as a function



		of root C stock, the coefficient being derived from GEM estimates; growth respiration calculated in SPA as $\text{root NPP} \times 0.28$
Respiration	output	sum of simulated leaf, wood and root respiration, evaluated against GEM data
GPP	output	generated through SPA process-based modelling of GPP using detailed parameters, evaluated against GEM data
NPP	output	calculated in SPA as GPP minus autotrophic respiration, evaluated against GEM data

1010

1015



1020 Table 3. Field estimated mean annual leaf area index (LAI), leaf traits, maximum rooting depth and fine root biomass for Amazon permanent sample plots along a MCWD gradient. LAI estimates were derived from monthly hemispherical photographs. LAI, leaf trait and rooting depth estimates were used to constrain SPA model runs. Estimate standard errors are presented in brackets. Fine root C stock estimates were absent for Tanguro plots.

	LAI ($\text{m}^2 \text{ m}^{-2}$)	LMA (g m^{-2})	leaf N content (g m^{-2})	Maximum Rooting Depth (m)	Fine Root C Stock (g C m^{-2})
CAX04	4.99 (± 1.07)	93 (± 17)	1.82 (± 0.43)	8	345
CAX06	5.23 (± 0.92)	87 (± 54)	2.12 (± 0.7)	10	433
TAM05	4.85 (± 0.81)	101 (± 24)	2.38 (± 0.56)	1	770
TAM06	4.64 (± 0.77)	96 (± 21)	2.51 (± 0.64)	1	500
KEN01	2.77 (± 0.17)	53 (± 13)	2.12 (± 0.25)	2	818
KEN02	2.22 (± 0.14)	42 (± 13)	2.31 (± 0.31)	1	607
Tanguro	4.13 (± 1.01)	64 (± 13)	2.01 (± 0.52)	<10	-

1025

1030



1035 Table 4. SPA calibrated leaf litterfall parameters for plots across an Amazon MCWD gradient. Peak leaf fall is the day of year leaf litterfall reaches its maximum, leaf lifespan reflects maximum lifespan of leaves and leaf fall period is the number of days over which systematic increases in leaf fall occur. Leaf litterfall parameters were calibrated against GEM field estimates to capture leaf litterfall and timing.

	Peak Leaf Fall (day of year)	Leaf Lifespan (years)	Leaf Fall Period (days)
CAX04	210	3.00	150
CAX06	190	1.45	100
TAM05	220	1.30	130
TAM06	230	1.42	100
KEN01	200	1.05	100
KEN02	180	1.01	100
Tanguro	180	1.04	120

1040

1045



Table 5. A comparison of GEM field measurements and SPA process-based modelling estimates of component autotrophic respiration and NPP. We present the R^2 , p-value, and root mean square error (RMSE) of the interaction between SPA and GEM annual estimates, together with the range in GEM biometrically derived estimates across seven sample plots at four locations in the Amazon basin.

Component	R^2	p-value	RMSE	Range in Field Estimates ($\text{gC m}^{-2} \text{yr}^{-1}$)
Respiration				
Foliage	0.47	0.09	92.0	454-830
Wood	0.75	0.01	100.5	411-1054
Fine Root	0.91	<0.001	74.1	232-1041
NPP				
Foliage	0.99	<0.001	9.0	150-491
Wood	0.21	0.30	25.3	189-292
Fine Root	0.59	0.04	49.5	189-418

1055

1060



1065 Table 6. The proportion of variation in GPP across seven GEM Amazonian permanent sample plots explained by photosynthetic drivers in SPA. Model drivers were alternated individually at each plot to that of all other plots and the resultant change in GPP retrieved. Proportion of variance explained was calculated as conditional sum of squares divided by the total sum of squares (n=476; where the conditions were LAI, photosynthetic capacity, rooting depth, root biomass, climate and soil).

Driver	Percentage of Variation Explained (%)
LAI	32.8
Photosynthetic capacity	21.3
Climate	16.2
Root depth	4.1
Soil	1.2
Root biomass	0.7

1070

1075



Table 7. The relative importance of LAI, VPD, solar radiation, precipitation and air temperature (T_{air}) in driving monthly variation in GPP (%). Monthly GPP estimates are derived from calibrated SPA simulations for seven permanent sample plots across an Amazon MCWD gradient, constrained using
1080 monthly field LAI measurements. Relative importance values were derived from analyses using the random forest technique ($n=168$).

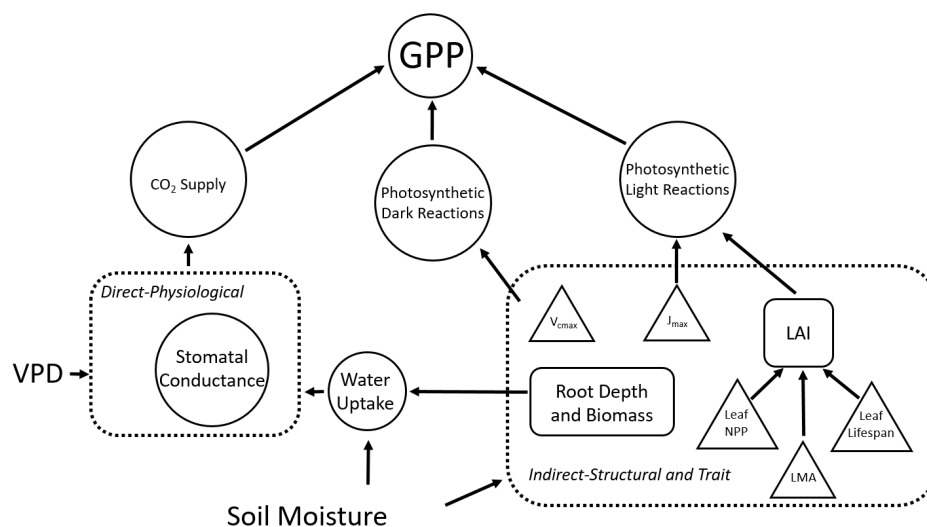
Plot	LAI	VPD	Solar Radiation	Precipitation	T_{air}
CAX04	13	17	58	8	5
CAX06	6	16	64	8	5
TAM05	17	22	53	3	5
TAM06	17	21	53	3	7
KEN01	16	21	45	10	8
KEN02	32	14	42	4	8
Tanguro	33	20	24	6	10

1085

1090



Figures



1095 Figure 1. A schematic of the direct and indirect effects of drought stress (via soil moisture and VPD on
 GPP. Drought stress affects GPP directly via stomatal conductance, and indirectly through its
 1100 determinant effect on plant traits and structural properties. Plant processes are represented by circles,
 traits are represented by triangles and vegetation properties (i.e. ecosystem structure) are represented
 by rectangles. Dashed boxes identify interactions driving the direct and indirect pathways through
 which drought stress impacts GPP. We note that other climate forcings (e.g. shortwave radiation and
 temperature) impact GPP but are not included here.

1105

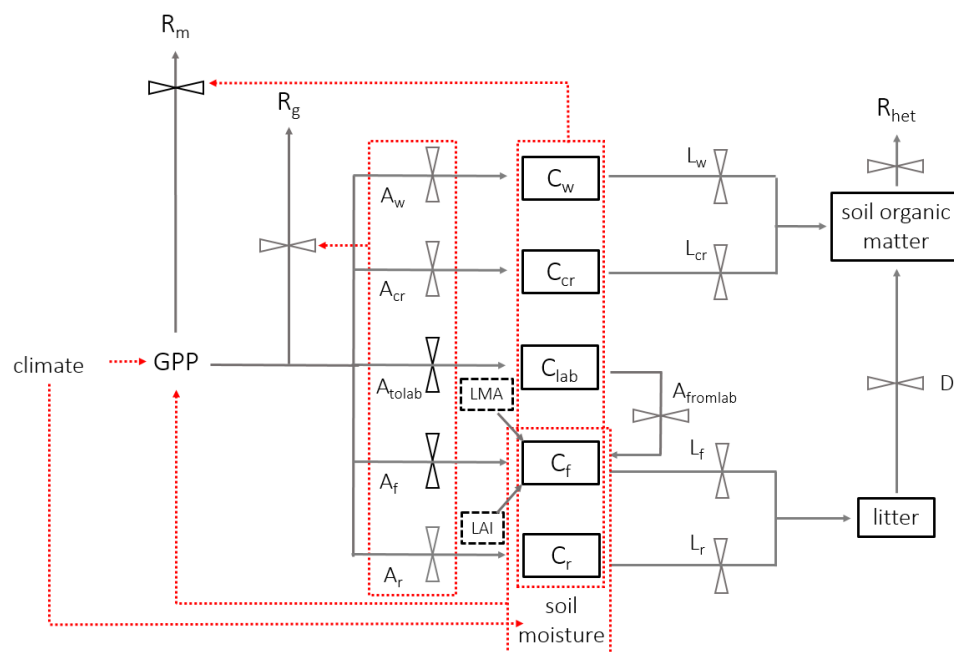


Figure 2. A schematic of DALEC_{canopy}, the carbon allocation sub-model integrated within the soil-plant-atmosphere model. Carbon moves between pools (solid boxes) via fluxes (solid arrows). Leaf carbon fluxes are constrained by field measurements (black dashed boxes). An effect of climate, carbon pools or fluxes on another carbon flux is shown by a red dashed arrow, whereby red dotted boxes indicate a collective impact of the contained carbon pools or fluxes. Black flux bars indicate that the carbon pathway is prioritised within the model above pathways from the same nodule. Climate is a model input, whilst soil moisture is simulated within SPA. Carbon pools (C), allocation (A) and litterfall (L) are separated by component: w = wood, cr = coarse roots, r = fine roots, f = foliage, lab = labile (or non-structural carbon), with to and from used for labile carbon.

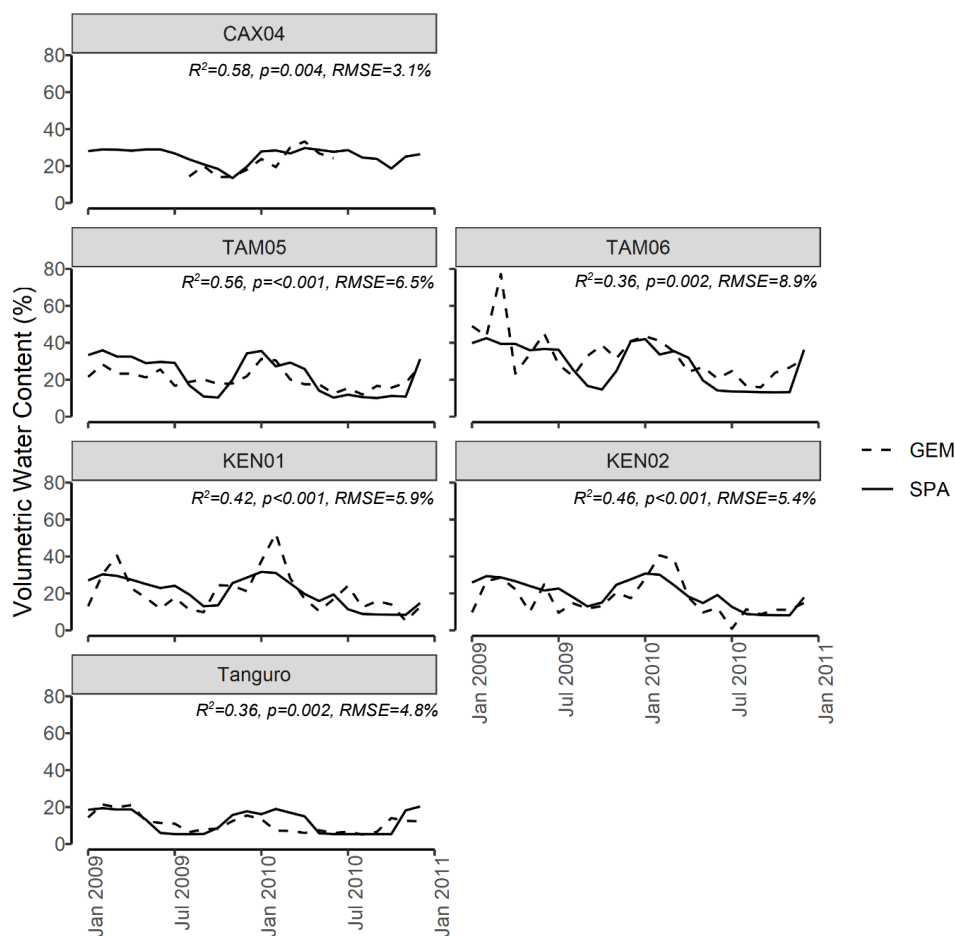
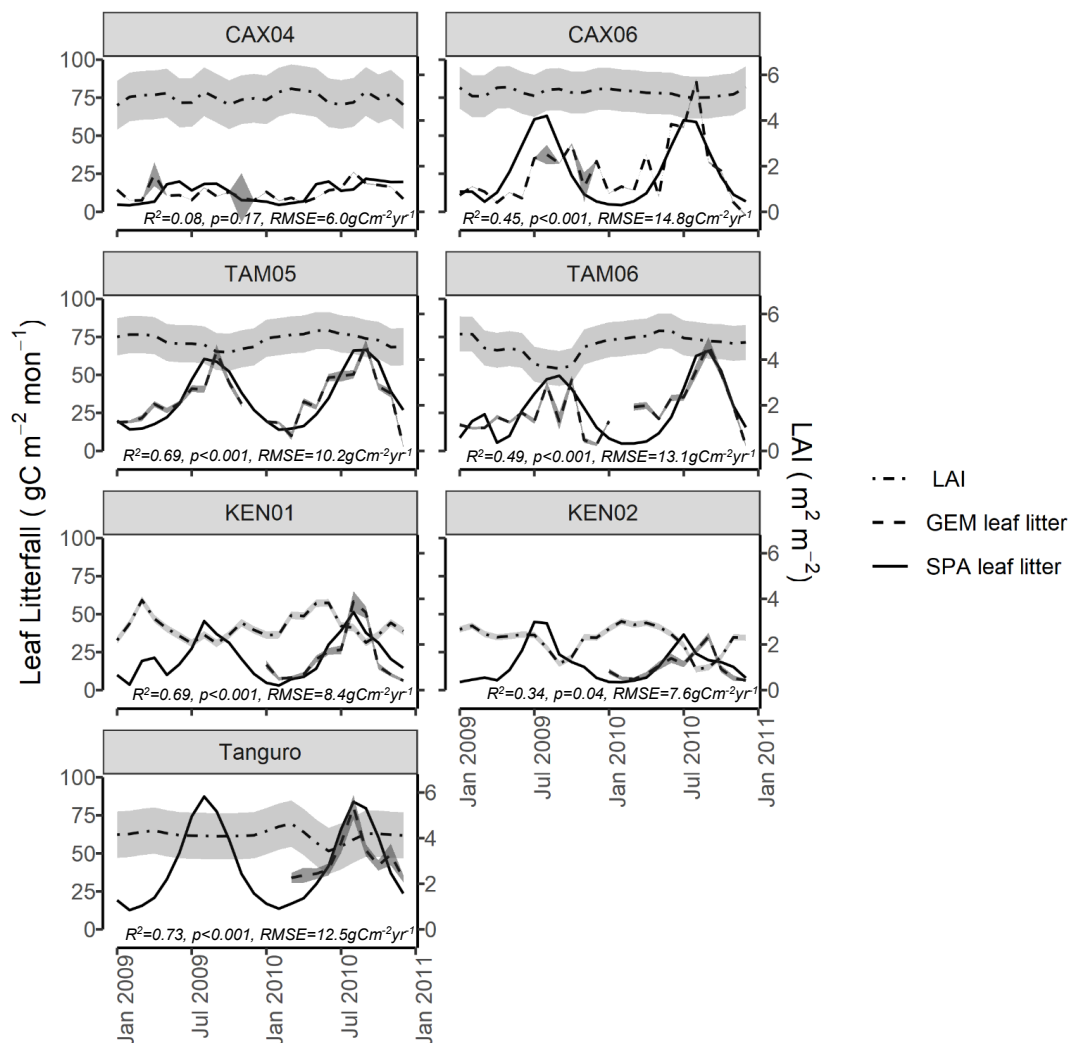


Figure 3. SPA estimated soil volumetric water content compared to GEM measured values for six of the seven sample plots at four locations across the Amazon basin. Data presented is for the time period 1120 2009-2010. Field data for CAX04 was limited to a shorter time period and for CAX06 was unavailable. R^2 , p-value and RMSE estimates presented are derived from linear regressions between monthly GEM measurements and SPA simulations.



1125 Figure 4. Field estimated monthly LAI, leaf litterfall (GEM), and standard error, compared with SPA
 1130 simulated leaf litterfall for seven plots at four locations across the Amazon basin. SPA leaf litterfall was
 calibrated against GEM estimates to derive three fixed model drivers relating to the leaf cycle (peak
 leaf fall timing, leaf fall period and leaf lifespan). GEM leaf litterfall data was available for 2009-2010
 for CAX04, CAX06, TAM05, TAM06 and for 2010 only for KEN01, KEN02 and Tanguro. R^2 , p -value
 and RMSE estimates presented are derived from linear regressions between monthly GEM
 measurements and SPA simulations.

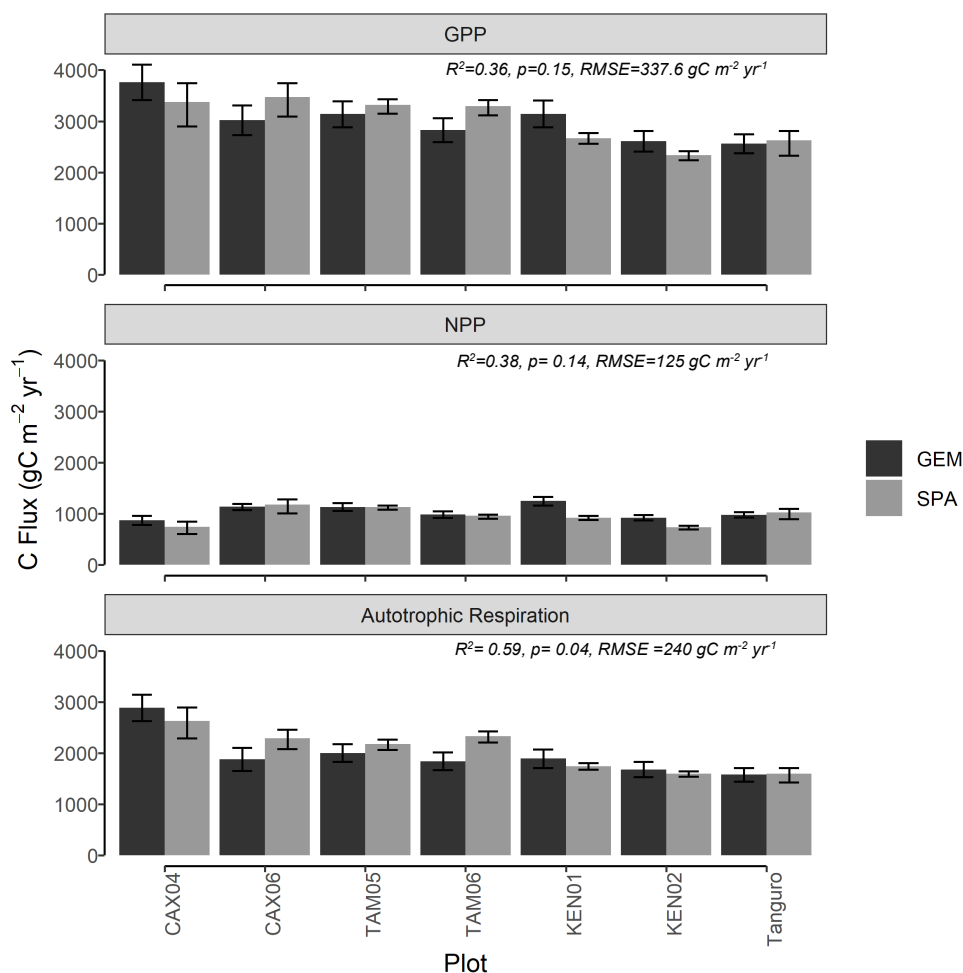


Figure 5. Carbon flux estimates ($\text{gC m}^{-2} \text{yr}^{-1}$) of (a) GPP, (b) NPP and (c) autotrophic respiration, derived
1135 from process-based modelling (SPA) and biometric methods (GEM) for seven permanent sample plots
at four locations across the Amazon basin. Estimates are mean annual values representative of the years
2009-2010. GEM error bars represent standard error from field carbon flux measurements. SPA error
bars represent simulated C fluxes under the upper and lower field LAI standard error. R^2 , p values and
RMSE represent the interaction between SPA and GEM C flux estimates.

1140



1145 Figure 6. The sensitivity of GPP to model driver alternations in SPA at each location. Model drivers LAI, climate (characterised by MCWD), photosynthetic capacity (characterised by V_{max}) and rooting depth, derived from field observations, were alternated individually at each plot to that of all other plots and the resultant GPP retrieved. Solid lines represent SPA simulated GPP under the named driver alternations, whilst the dashed line represents the simulated value under observed conditions. SPA GPP



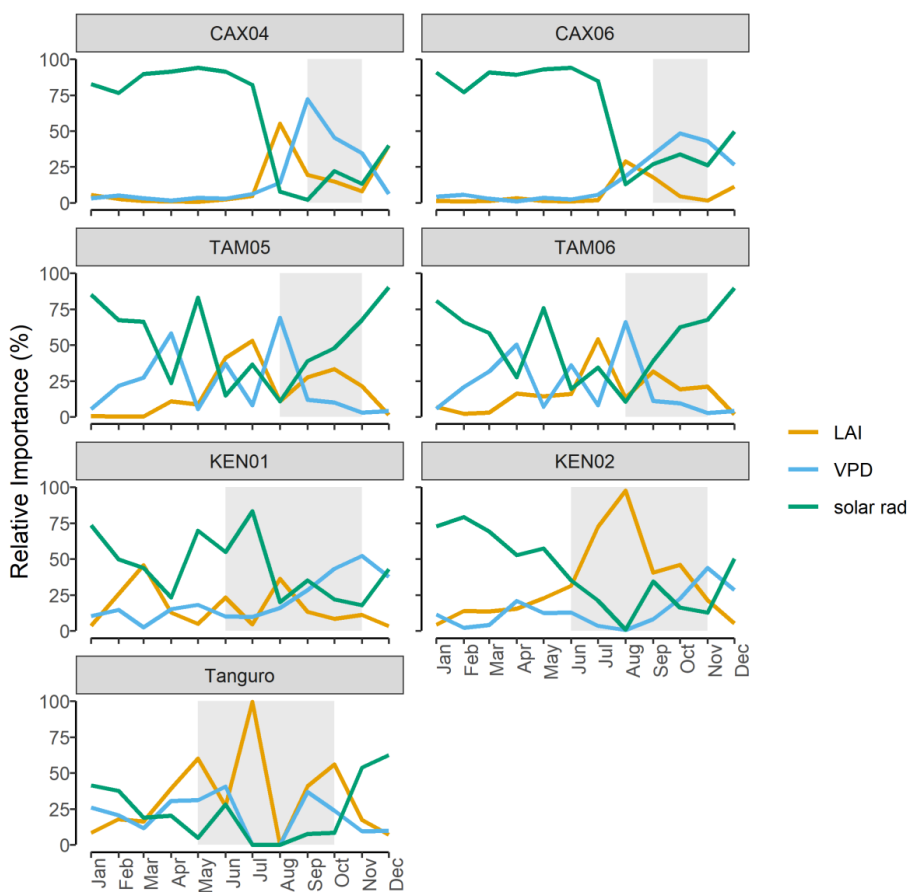
1150 estimates presented are location averages. Climate and LAI were input to the model as timeseries, whilst
photosynthetic capacity and rooting depth were fixed values. Plots are ordered to reflect soil moisture-
stress which increases from Caxiuanã > Tambopata > Kenia > Tanguro.

1155

1160

1165

1170



1175 Figure 7. The relative importance (%) of LAI, vapour pressure deficit (VPD) and solar radiation (solar rad) in driving SPA estimated monthly photosynthesis at permanent sample plots across an Amazon MCWD gradient. Relative importance was calculated using random forest machine learning. Shaded regions represent the dry season, where monthly precipitation was below 100mm. Plots are ordered to reflect drought stress which increased from Caxiuanã to Tambopata to Kenia to Tanguro.